HHS Public Access

Author manuscript

Sci Transl Med. Author manuscript; available in PMC 2023 September 14.

Published in final edited form as:

Sci Transl Med. 2023 March ; 15(685): eabm5663. doi:10.1126/scitranslmed.abm5663.

Soluble CTLA-4 mutants ameliorate immune-related adverse events but preserve efficacy of CTLA-4– and PD-1–targeted immunotherapy

Mingyue Liu[1,†], **Xu Wang**[1,†], **Xuexiang Du**[1,2,†], **Wei Wu**[1,3], **Yan Zhang**[1,4], **Peng Zhang**[1,5], **Chunxia Ai**[1,2], **Martin Devenport**[3], **Juanjuan Su**[1,3], **Musleh M. Muthana**[1], **Lishan Su**[1,6], **Yang Liu**[1,3,*], **Pan Zheng**[1,3,*]

[1]Division of Immunotherapy, Institute of Human Virology and Department of Surgery, University of Maryland School of Medicine, Baltimore, MD 21201, USA

[2]Key Laboratory of Infection and Immunity of Shandong Province & Department of Immunology, School of Basic Medical Sciences, Shandong University, Jinan, 250012, China

[3]OncoC4 Inc., Rockville, MD 20805, USA

[4]Department of Immunology and Microbiology, State Key Laboratory of Oncogenes and Related Genes, Shanghai Institute of Immunology, Shanghai Jiao Tong University School of Medicine, Shanghai 200025, China

[5]Beijing Key Laboratory for Genetics of Birth Defects, Beijing Pediatric Research Institute, Beijing Children's Hospital, Capital Medical University, National Center for Children's Health, Beijing 100045, China

[6]Laboratory of Viral Pathogenesis and Immunotherapy, Divisions of Virology, Pathogenesis and Cancer and Immunotherapy, Institute of Human Virology and Department of Pharmacology, University of Maryland School of Medicine, Baltimore, MD 21201, USA

Abstract

*Corresponding author. yangl@oncoc4.com (Y.L.); pzheng@oncoc4.com (P.Z.).
†These authors contributed equally to this work.

Author contributions: M.L., X.W., and X.D. designed the study, performed the bulk of the experiments, and analyzed the data. P. Zheng, Y.L., and L.S. designed and supervised the research. C.A. and Y.Z. assisted with experiments associated with the tumor models and irAE models. W.W. established the method to evaluate the binding of CTLA-4 mutants to hB7-1/B7-2 and anti–CTLA-4 antibodies. J.S. and M.M.M. helped collect the tissues for irAE evaluation. P. Zhang performed bioinformatics and statistical analyses. M.L. and Y.L. wrote the paper with input from other coauthors. M.D. reviewed and edited the manuscript.

Competing interests: P.Zheng and Y.L. are cofounders of and have equity interest in OncoC4 Inc. M.D. is the Chief Operating Officer at OncoC4 and has equity interest in OncoC4 Inc. Y.L. P. Zheng, M.D., W.W., X.D., and M.L. are inventors on a U.S. patent (17/677,795) application titled "CD80 and CD86 binding protein compositions and uses thereof." All other authors declare that they have no competing interests.

Supplementary Materials
This PDF file includes:
Figs. S1 to S11
Table S1
Other Supplementary Material for this manuscript includes the following:
Data file S1
MDAR Reproducibility Checklist
View/request a protocol for this paper from Bio-protocol.

Immune checkpoint inhibitors (ICIs), such as nivolumab and ipilimumab, not only elicit antitumor responses in a wide range of human cancers but also cause severe immune-related adverse events (irAEs), including death. A largely unmet medical need is to treat irAEs without abrogating the immunotherapeutic effect of ICIs. Although abatacept has been used to treat irAEs, it risks neutralizing the anti–cytotoxic T lymphocyte–associated protein 4 (CTLA-4) monoclonal antibodies administered for cancer therapy, thereby reducing the efficacy of anti–CTLA-4 immunotherapy. To avoid this caveat, we compared wild-type abatacept and mutants of CTLA-4–Ig for their binding to clinically approved anti–CTLA-4 antibodies and for their effect on both irAEs and immunotherapy conferred by anti–CTLA-4 and anti–PD-1 antibodies. Here, we report that whereas abatacept neutralized the therapeutic effect of anti–CTLA-4 antibodies, the mutants that bound to B7-1 and B7-2, but not to clinical anti-CTLA-4 antibodies, including clinically used belatacept, abrogated irAEs without affecting cancer immunotherapy. Our data demonstrate that anti–CTLA-4–induced irAEs can be corrected by provision of soluble CTLA-4 variants and that the clinically available belatacept may emerge as a broadly applicable drug to abrogate irAEs while preserving the therapeutic efficacy of CTLA-4–targeting ICIs.

INTRODUCTION

Cytotoxic T lymphocyte–associated protein 4 (CTLA-4)– and programmed cell death protein 1 (PD-1)/programmed cell death ligand 1 (PD-L1)–targeted immune checkpoint inhibitors (ICIs) are the most important developments in cancer therapy over the past decade because they provide curative therapies for multiple types of cancers. However, ICI immunotherapies are associated with a wide spectrum of immune-related adverse events (irAEs) that can cause damage to essentially all organs and tissues with varying frequencies and severities. Combined PD-1– and CTLA-4–targeted immunotherapy comprising nivolumab and ipilimumab substantially increases the objective response rates and patient survival in multiple types of cancers (1–5), although this comes at the cost of more frequent and serious irAEs than monotherapy. The incidence of severe irAEs (grade 3 or 4) reached 50 to 90%, depending on the therapeutic setting (2, 6–9); among them, the mortality rate of myocarditis is about 45% (10).

In addition to the effects on health, irAEs also prevent immunotherapy from reaching its full clinical efficacy. For instance, clinical pharmacology studies suggest that the currently approved dosing regimen of ipilimumab falls well short of what is required for optimal therapeutic efficacy (11). The inadequate dosing of ipilimumab partially explains why CTLA-4 targeting underperforms compared with PD-1/PD-L1–targeting immunotherapy. Therefore, ameliorating irAEs associated with anti–CTLA-4 immunotherapy may provide a way to improve the therapeutic effect of this ICI.

A critical issue in combating anti–CTLA-4–induced irAEs is the need to understand the underlying mechanism causing them. Our previous studies have demonstrated that CTLA-4–targeting antibodies, including ipilimumab and Treme-IgG1, an immunoglobulin G1 (IgG1) version of tremelimumab, trigger irAEs by causing lysosomal degradation of CTLA-4 (12), which phenocopies the genetic inactivation of *CTLA4* or *LRBA* in humans (13). Human autoimmune diseases caused by *CTLA4* mutation were successfully treated with abatacept,

which is a soluble CTLA-4 fusion protein consisting of the wild-type extracellular domains of CTLA-4 and the Fc of human IgG1 (13). Recently, another group also reported that abatacept rescued myocarditis in the *Ctla4*$^{+/-}$ *Pdcd1*$^{-/-}$ mouse model (14). Therefore, it is of interest to consider whether a similar approach can be adopted for the treatment of irAEs. Consistent with this notion, it has been reported that a patient with corticosteroid-refractory ICI-associated myocarditis was successfully treated with abatacept (15).

Several issues must be resolved before successful deployment of soluble CTLA-4 as a treatment for irAEs. The first and the most obvious is that abatacept and anti–CTLA-4 antibodies are mutually antagonistic, and, hence, it is difficult to envision that abatacept would treat irAEs while preserving the antitumor efficacy of anti–CTLA-4 antibodies. Second, it is unclear whether anti–CTLA-4 antibodies retain immunotherapeutic activity if the T cell priming activity of B7-1 and B7-2 through CD28 is blocked by soluble CTLA-4. This would be achievable if the function of anti–CTLA-4 is to cause depletion of regulatory T (T_{reg}) cells in the tumor through antibody-dependent cellular cytotoxicity/phagocytosis (ADCC/ADCP) (16–19) and if soluble CTLA-4 does not neutralize anti–CTLA-4 antibodies. To address both issues, we generated a series of CTLA-4 variants and evaluated their binding to clinically tested irAE-prone anti–CTLA-4 antibodies. We found that, unlike the wild-type soluble CTLA-4 fusion protein abatacept, several variants retained binding to B7-1 and B7-2 but lost binding to clinically used anti–CTLA-4 antibodies. These variants ameliorate irAEs without negatively affecting the cancer therapeutic effect, even when coadministrated with anti–CTLA-4 antibodies. Because one of the most potent variants is belatacept, which has been approved for human use, our data provide an approach to treating irAEs with the potential for rapid translation to clinical practice.

RESULTS

Screening for soluble CTLA-4 mutants that bind to B7, but not to anti–CTLA-4, antibodies

There are two criteria for applying CTLA-4–Ig to ameliorate irAEs in patients with cancer. One is that the CTLA-4–Ig fusion protein should have good binding ability to B7-1 and B7-2 molecules; the other is the CTLA-4–Ig fusion protein cannot neutralize anti–-CTLA-4 monoclonal antibodies (mAbs), especially the clinically used drug ipilimumab. Human CTLA-4 (hCTLA-4) and mouse CTLA-4 molecules are functionally conserved in ligand binding (20) (21). Because of immune tolerance, mouse CTLA-4 should not bind to most anti–CTLA-4 antibodies that were produced by immunizing mice with hCTLA-4 molecules. We therefore reasoned that, by replacing clusters of amino acids unique to hCTLA-4 protein with their murine counterparts, we may generate fusion proteins that would be functional in both mice and humans but not reactive with anti–hCTLA-4 mAbs. On the basis of this notion, we engineered a series of hCTLA-4–Ig mutants (M1 to M14, M16, and M17) as candidates for irAE treatment (table S1). Together with the two clinical drugs, abatacept (wild-type CTLA-4–Ig) and belatacept (CTLA-4–Ig variant), we screened for their binding activity to human B7-1 (hB7-1)/hB7-2 and anti–CTLA-4 mAbs. We immobilized CTLA-4–Ig on a plate and detected binding by serial dilution of biotinylated hB7-1 or hB7-2 (Fig. 1, A and B, and fig. S1, A and B). We found that among all tested CTLA-4–Ig fusion proteins, belatacept had the highest binding ability to both hB7-1 and hB7-2 molecules. Abatacept,

M12, M13, M14, M16, and M17 also showed evidence of binding. Then, we evaluated the interaction between CTLA-4-Ig and ipilimumab. Although abatacept showed the highest binding ability to ipilimumab, belatacept, M10, M11, and M17 did not bind to ipilimumab (Fig. 1C and fig. S1C). Belatacept and M17 were thus good candidates, with high binding to B7 and low binding to ipilimumab. To broaden the potential application, we also detected their binding to the IgG1 variant of tremelimumab (Treme-IgG1), the other anti–CTLA-4 mAb approved for clinical use (Fig. 1D and fig. S1D). Again, belatacept demonstrated a lack of binding. Because M17 has weak binding to Treme-IgG1, we further modified M17 and generated four mutants, called M17-1, M17-2, M17-3, and M17-4, respectively. We found that M17-2 met all the requirements for hB7-1/B7-2 binding without binding anti–CTLA-4 (Fig. 1, E to G). On the basis of all these assays, we selected belatacept and M17-2 as candidates for further studies.

To compare the CTLA-4 fusion proteins for their effect on the interaction between ipilimumab and CTLA-4 molecules on the cell surface, we incubated anti-CD3/CD28–activated human T_{reg} cells with Alexa Fluor 488 (AF488)–conjugated ipilimumab in the presence of serial dilutions of abatacept, belatacept, M17-2, or control hIgFc. Abatacept blocked the binding of ipilimumab to T_{reg} cells in a dose-dependent manner, whereas belatacept and M17-2 had no blocking effect (Fig. 1H). All three CTLA-4 fusion proteins interrupted the interaction between hB7-1/B7-2 with hCTLA-4 (Fig. 1I) or human CD28 (hCD28) (Fig. 1J). We also evaluated the blocking effect of CTLA-4–Ig fusion proteins on CTLA-4–mediated trans-endocytosis of cell surface B7-1/B7-2 (Fig. 1, K and L). Consistent with their stronger inhibition of CTLA-4 binding to B7-1 and B7-2, belatacept and M17-2 were more efficient than abatacept in blocking CTLA-4–mediated trans-endocytosis.

Binding of CTLA-4–Ig fusion proteins to murine proteins was also evaluated, and all three proteins were bound to both murine B7-1 (mB7-1) and mB7-2. The data showed that the mutant fusion proteins had lower binding to mB7-1 and somewhat lower binding to mB7-2 (fig. S2, A and B). Although at lower efficacies than abatacept, both belatacept and M17-2 also efficiently inhibited murine CD28 (mCD28) to their ligands (fig. S2, C and D), respectively, with half-maximal inhibitor concentrations (IC_{50}) of 0.086 and 0.396 μg/ml for the mB7-1–mCD28 interaction and 5.787 and 1.127 μg/ml for the mB7-2–mCD28 interaction (fig. S2E). Our treatment regimens were able to deliver through concentrations of fusion proteins at 72 hours after each dosing that exceeded the IC_{50} values (fig. S2F). To evaluate CTLA-4–Ig fusion proteins for their effect on mouse T cell activation, we stimulated splenocytes from human *CTLA4* knock-in (*CTLA4*$^{h/h}$) mice with anti-CD3 mAb in the presence of varying concentrations of abatacept, belatacept, or M17-2. All three CTLA-4–Ig fusion proteins inhibited $CD4^+$ and $CD8^+$ T cell proliferation and their production of interferon-γ (IFN-γ) and tumor necrosis factor–α in a dose-dependent manner (fig. S3, A to D). The cross-reactivity and functional inhibition of the mouse B7-CD28 interaction allowed us to test the function of this CTLA-4-Ig in vivo.

Soluble CTLA-4 mutants preserve the therapeutic effect of ipilimumab

Given the role of B7-CD28 signaling in T cell priming, blocking B7 may interfere with the therapeutic effect of immunotherapy. However, many patients with cancer are known to

have developed T cell responses, which are restrained either by T_{reg} suppression or immune exhaustion. Hence, costimulation by B7 may be less critical once the T cell response has been initiated. To test whether CTLA-4–Ig impedes tumor rejection induced by anti–CTLA-4 mAbs, we inoculated adult *CTLA4*$^{h/h}$ mice subcutaneously with the colon cancer cell line MC38. When tumors reached a size of 5 to 7 mm in diameter, the mice were treated four times with 100 μg of ipilimumab together with CTLA-4–Ig fusion proteins or hIgFc every 3 days (Fig. 2A). Because M17-2 demonstrated faster clearance from the serum in mice (fig. S2F), the M17-2 dose was adjusted to achieve similar in vivo exposure. As expected, abatacept totally abolished the therapeutic effect induced by high doses of ipilimumab (100 μg per injection) that would normally induce complete tumor rejection. However, neither belatacept nor M17-2 adversely affected the tumor rejection by ipilimumab. To rule out the possibility that excessive ipilimumab may abrogate the negative impact of CTLA-4 mutants on tumor rejection, we decreased the dosage of ipilimumab to 10 μg per injection, which allowed tumor relapse (Fig. 2B). Again, belatacept and M17-2, but not abatacept, preserved the antitumor effect of ipilimumab. Similar results were obtained with the T lymphoma EG7 tumor model (Fig. 2C).

Because most patients who received ipilimumab also receive anti–PD-1 antibodies, it is of interest to test whether CTLA-4 fusion proteins impede the therapeutic effect of anti–PD-1 antibodies. To achieve this goal, we treated MC38 tumor–bearing mice with anti–PD-1 mAb (RMP1-14) in conjunction with abatacept, belatacept, or hIgFc. Neither abatacept nor belatacept affected tumor inhibition induced by anti–PD-1 (Fig. 2D). Clinically, combination therapy of ipilimumab and nivolumab is more effective than monotherapy (4, 22, 23). We therefore evaluated the impact of CTLA-4–Ig on combination therapy in the B16 melanoma model (Fig. 2E). We found that belatacept did not diminish the therapeutic effect induced by ipilimumab and anti–PD-1 mAb, whereas abatacept completely impaired the tumor inhibition.

To mimic the clinical scenario, we treated the tumor-bearing mice with ipilimumab first and then administered CTLA-4–Ig fusion proteins or hIgFc 3 days later (Fig. 2F). Belatacept and M17-2 did not affect tumor rejection, whereas abatacept abrogated tumor rejection in this setting. As expected, the impact of abatacept was reduced but remained significant ($P = 0.026$; $P < 0.001$) when administered 6 or 9 days after ipilimumab therapy (Fig. 2G), when tumor rejection has already been initiated.

We have reported in the *CTLA4*$^{h/h}$ mice that the therapeutic effect of ipilimumab depends on the ADCC/ADCP-mediated depletion of CTLA-expressing intratumoral T_{reg} cells (16). This effect may be preserved even if B7-CD28 interaction is disrupted by CTLA-4 fusion proteins, providing that the B7-CD28 interaction is no longer necessary for tumor immunity at the time when treatment of irAEs becomes necessary. To investigate the role of B7 in tumor immunotherapy in relation to anti–CTLA-4 treatment, we used anti–B7-1 (1G10) and anti–B7-2 (GL1) mAbs to block the B7-CD28 interaction (Fig. 2H). Consistent with our previous report, if anti-B7 mAbs were delivered before tumor inoculation or ipilimumab treatment, then the therapeutic effect induced by ipilimumab was completely abrogated. However, when administered concurrently with ipilimumab, anti-B7 mAbs did not affect the antitumor activity. These data are consistent with the hypothesis that B7 molecules are

required for induction of T cell priming but not after induction of tumor-reactive T cells. To determine whether CTLA-4–Ig mutant treatment affects established antitumor immunity, mice that achieved complete tumor regression after ipilimumab + hIgFc, belatacept, or M17-2 treatment were rechallenged with 4×10^6 MC38 cells (five times more cells than the primary tumor inoculation) after primary tumors had not been detected for more than 2 months (Fig. 2I). We found that all mice completely rejected the rechallenged tumors. Collectively, these data suggested that CTLA-4–Ig variants belatacept and M17-2 preserved the therapeutic effect induced by ipilimumab and anti–PD-1 mAbs in tumor-bearing mice, whereas abatacept abrogated the antitumor efficacy induced by ipilimumab.

Belatacept and M17-2 preserve T cell activation in the tumor microenvironment

To analyze the tumor microenvironment and further evaluate the impact of CTLA-4–Ig on antitumor immunity, we treated MC38-bearing mice with ipilimumab concurrently with abatacept, belatacept, M17-2, or hIgFc on days 10, 13, and 16 and then harvested tumor masses for flow cytometry analysis on day 19. Given the critical role of T_{reg} depletion in anti–CTLA-4 mAb therapy (17–19), we assessed the percentage of T_{reg} cells among $CD4^+$ T cells in the tumor microenvironment. There was an abundance of T_{reg} infiltration in tumors of the control group, which was largely depleted by ipilimumab (Fig. 3, A and B). As expected, abatacept completely abrogated ipilimumab-induced T_{reg} depletion, whereas belatacept and M17-2 did not inhibit T_{reg} depletion. Similar observations were made with the B16 and EG7 tumor models (fig. S4). Consistent with a less potent therapeutic effect of anti–CTLA-4 mAbs in these models (16, 24), T_{reg} cell depletion by ipilimumab was less robust when compared with the MC38 model (fig. S4). Ipilimumab treatment increased the total number of $CD8^+$ T cells that produced IFN-γ or granzyme B in the tumor microenvironment (Fig. 3, C and D). Whereas abatacept abolished IFN-γ and granzyme B production, belatacept and M17-2 preserved the ipilimumab-induced activation of $CD8^+$ T cells. Furthermore, ipilimumab therapy reduced the percentage of $PD\text{-}1^+$, and T cell Ig and mucin domain 3 ($Tim\text{-}3^+$) exhausted $CD8^+$ T cells in the tumor microenvironment; this reduction was abrogated by abatacept, but not by either belatacept or M17-2 (Fig. 3, E and F).

To confirm the biological activity of belatacept and M17-2, we examined their impact on T cell function in draining lymph nodes. We found that although ipilimumab increased the IFN-γ–expressing $CD4^+$ and $CD8^+$ T cells, it did not increase granzyme B expression in either cell type (Fig. 3, G to J). Because abatacept neutralizes ipilimumab, it abrogated the effect of ipilimumab on IFN-γ expression in T cells as expected. In contrast, the amount of ipilimumab used was insufficient to fully neutralize the effect of abatacept, because granzyme B–expressing $CD4^+$ cells in the ipilimumab + abatacept group were lower than those found in control IgFc-treated mice. Because belatacept and M17-2 also reduced IFN-γ– and granzyme B–expressing $CD4^+$ cells to similar extents, they were biologically active in the draining lymph nodes.

B7-1 and B7-2 are required for the antibody response to antigens (25). Because anti–CTLA-4 mAbs are potent inducers of antidrug antibodies (ADAs) in mice, ADA is a good indicator for the function of both B7-1 and B7-2 in vivo. To test whether both

abatacept and belatacept efficiently block B7 signaling in vivo, we evaluated ADAs induced by ipilimumab. Both drugs completely abrogated ADAs in vivo (fig. S5). Although both abatacept and belatacept completely abrogated ipilimumab-induced antibody responses, they likely achieved the effect through different mechanisms, because abatacept may neutralize ipilimumab and block B7, whereas belatacept only works through blocking B7. Together, our data demonstrated that in tumor-bearing mice, all CTLA-4 fusion proteins tested interfere with the function of endogenous B7 costimulation. However, abatacept, but not belatacept or M17-2, interfered with the therapeutic effect of anti–CTLA-4 antibodies.

CTLA-4–Ig variants inhibit irAEs prophylactically and therapeutically

We have reported that treatment of very young human *CTLA4* knock-in ($CTLA4^{h/h}$) mice with ipilimumab and anti-mouse PD-1 mAb faithfully recapitulates multiple irAEs observed with the clinical use of ipilimumab and nivolumab (24). To evaluate the impact of CTLA-4–Ig mutants on irAEs, we treated $CTLA4^{h/h}$ mice with ipilimumab and anti–PD-1 in conjunction with hIgFc or soluble CTLA-4 mutants on days 10, 13, 16, and 19 after birth. The rate of body weight gain was evaluated over time, and hematologic and histopathologic alterations were evaluated at 6 weeks of age (Fig. 4A). Combination of ipilimumab and anti–PD-1 resulted in substantial growth retardation. However, mice treated with belatacept or M17-2 showed normal body weight gain compared with the control group (Fig. 4B and fig. S6A). To study the impact of CTLA-4 mutants on red blood cell anemia induced by combination therapy, we performed complete blood count (CBC) analysis at 1 month after the initiation of therapy. We observed a significant ($P = 0.001$; $P < 0.001$; $P < 0.001$) reduction of red blood cell (RBC) counts, blood hematocrit (HCT), and total hemoglobin (Hb) among the mice treated with ipilimumab and anti–PD-1, whereas those that received belatacept or M17-2 treatment had normal hematopoiesis (Fig. 4C and fig. S6B).

Myocarditis is a rare irAE associated with ICI immunotherapy but is among the most severe (26–29). Our previous study showed that ipilimumab + anti–PD-1 treatment resulted in enlarged hearts in $CTLA4^{h/h}$ mice (24). Eight of 18 ipilimumab + anti–PD-1–treated mice had a heart weight greater than 1% of their body weight, whereas none of the ipilimumab + anti–PD-1 + belatacept–treated mice showed this enlargement (Fig. 4D). Myocarditis was confirmed by massive lymphocyte infiltration in the endocardium and myocardium in the ipilimumab + anti–PD-1–treated mice; consistent with the data on heart weight, treatment with belatacept or M17-2 significantly ($P < 0.001$) decreased evidence of myocarditis (Fig. 4, E and F, and fig. S6C).

Similar prophylactic effects of belatacept and M17-2 were observed in other organs. Although the combination of ipilimumab and anti–PD-1 induced severe inflammation in all major organs of most mice, belatacept and M17-2 significantly ($P < 0.001$) decreased tissue inflammation to mild or moderate degrees (Fig. 4, E and F, and fig. S6C). When the scores from all organs were combined, the protective effects of belatacept and M17-2 on irAEs were more noteworthy (Fig. 4G and fig. S6D). Together, soluble CTLA-4 mutants inhibited ipilimumab, and anti–PD-1 treatment induced irAEs, including red blood cell anemia, myocarditis, and multiple organ inflammation.

To test whether the fusion proteins have a therapeutic effect against established irAEs, we treated *CTLA4*$^{h/h}$ mice with four injections of ipilimumab and anti–PD-1 to induce irAEs and initiated treatment with belatacept when growth retardation was observed (Fig. 5A). We found that, despite an initial delay, belatacept restored mouse growth to degrees found in the control group (Fig. 5B).

We also followed the mice for 120 days to assess the survival benefit after treatment with mutant CTLA-fusion proteins. Whereas 40% ipilimumab + anti–PD-1–induced mice died within 3 months when they received only control IgGFc, all mice that received either belatacept or M17-2 survived the ipilimumab + anti–PD-1–induced irAEs (Fig. 5C). Moreover, although ipilimumab + anti–PD-1 induced severe anemia in the IgGFc control group, no mice developed anemia after belatacept treatment (Fig. 5D). In addition, belatacept also protected ipilimumab + anti–PD-1–induced mice against heart enlargement (Fig. 5E). Histological analysis showed that belatacept significantly ($P < 0.001$) inhibited the inflammation in heart, salivary gland, and lung (Fig. 5, F to H). Although decreased inflammation in the liver was not observed, fewer mice treated with belatacept after combination of ipilimumab and anti–PD-1 therapy developed abnormally high alanine transaminase (ALT) concentrations (>100 U/liter) as compared with the control group (fig. S7). The mice that survived ipilimumab + anti–PD-1 treatment were also phenotypically normal over the long term when evaluated by standard toxicity measures (fig. S8). We used high doses of CTLA-4 fusion proteins for the evaluation of safety and observed no changes in body weight (fig. S9A) or liver damage (fig. S9B). Further, no adverse hematological observations were found (fig. S9C).

Because tremelimumab was recently approved by the U.S. Food and Drug Administration for cancer treatment in combination with an anti–PD-L1 antibody, we tested whether belatacept or M17-2 could be used in Treme-IgG1 therapy. In combination with anti–PD-1 mAb, Treme-IgG1 induced a robust growth retardation, but both belatacept and M17-2 efficiently restored body weight (fig. S10A). The CTLA-4 mutants also rescued the red blood cell anemia (fig. S10B) and multiple organ inflammation (fig. S10, C and D) induced by Treme-IgG1 and anti–PD-1 therapy. These results indicate that these CTLA-4 mutant fusion proteins have promising prophylactic and therapeutic effects on irAEs induced by dual CTLA-4— and PD-1–targeting therapies and a strong safety profile to support clinical use.

Belatacept and M17-2 reduce T cell infiltration and activation in irAE target organs

It is increasingly clear that the cancer immunotherapeutic effect of anti–PD-1 and anti–CTLA-4 correlates, respectively, with the normalization of T cell function (30) and intratumoral T_{reg} depletion (16, 31). In contrast, irAEs correlate with systemic T cell activation and associated toxicity outside of the tumor. To further understand the mechanism of the protective effect of CTLA-4 mutants against irAEs, we analyzed the frequency and functional subsets of T cells in peripheral blood in our irAE model. The frequencies of $CD4^+$ T cells were comparable in all groups (Fig. 6A). The frequency of $CD8^+$ T cells in the peripheral blood was significantly ($P = 0.003$) increased after ICI therapy, but this was decreased in mice treated with CTLA-4 mutant proteins (Fig. 6B). Ipilimumab significantly

($P < 0.001$) increased the T_{reg} frequency in the blood (Fig. 6C), which is consistent with clinical observation (32), but this was inhibited by belatacept and M17-2 treatment, presumably because CD28 is needed for maintenance of T_{reg} cells (33, 34). We next evaluated peripheral T cell function through intracellular staining of IFN-γ. Ipilimumab + anti–PD-1 treatment induced a significant ($P < 0.001$) increase in IFN-γ production in both $CD4^+$ and $CD8^+$ T cells (Fig. 6D). Belatacept and M17-2 inhibited the cytokine production in $CD4^+$, but not $CD8^+$, T cells. By cell surface phenotype, a substantial expansion of effector memory T cells ($CD44^{hi}$ $CD62L^{lo}$) was observed after ipilimumab + anti–PD-1 treatment in both the $CD4^+$ and $CD8^+$ T cell populations (Fig. 6, E and F). Correspondingly, the frequencies of naïve T cells ($CD44^{lo}$ $CD62L^{hi}$) were significantly ($P < 0.001$) reduced. Belatacept and M17-2 decreased the frequency of effector memory T cells while increasing the frequency of naïve T cells. Because loss of naïve T cells and increase in effector memory T cells correlated with multiple organ inflammation (24), these data suggest that CTLA-4 variants protect against irAEs through inhibiting systemic $CD4^+$ and $CD8^+$ T cell activation.

To further explore how CTLA-4–Ig fusion proteins affected the irAE-targeted organs, we performed flow cytometry analysis of the cell populations and functions in hearts and livers. There was a massive accumulation of $CD45^+$ cells in both hearts (Fig. 7A) and livers (Fig. 7B) after combination therapy, but treatment with belatacept or M17-2 markedly decreased this immune cell infiltration. Among all the cell subpopulations, $CD4^+$ and $CD8^+$ T cells were the most increased after immunotherapy and decreased after CTLA-4–Ig fusion protein treatment (Fig. 7, A and B, and fig. S11). Corresponding to increased T cell infiltration, T_{reg} densities were increased after ICI therapy in both hearts and livers, although the frequency of T_{reg} cells among $CD45^+$ cells was actually decreased in the heart. The natural killer (NK) cell density increased in the heart, whereas it decreased in the liver. However, the percentage of NK cells in $CD45^+$ cells slightly decreased in the heart and significantly ($P < 0.001$) decreased in the liver (fig. S11). B cells and myeloid cells had no change in cell numbers.

Because T cells are the major cell populations contributing to tissue inflammation, next we examined the function of liver-infiltrating T cells. We found that anti–CTLA-4 + anti–PD-1 treatment robustly increased the frequency of IFN-γ–expressing $CD4^+$ T cells, whereas belatacept and M17-2 markedly decreased these populations (Fig. 7C). There was no change in the frequency of granzyme B–, interleukin-4 (IL-4)–, or IL-17A–producing $CD4^+$ T cells. In addition, neither IFN-γ nor granzyme B production of $CD8^+$ T cells was affected by ICI therapy (Fig. 7D). Collectively, these results suggest that $CD4^+$ and $CD8^+$ T cells in peripheral tissues, especially IFN-γ–expressing $CD4^+$ T cells, contribute to irAEs, because CTLA-4 mutant fusion protein treatment was associated with lower frequencies of these cells in target organs.

DISCUSSION

Severe irAEs represent a major medical challenge in the face of widespread adoption of immunotherapy, especially PD-1/CTLA-4 dual-targeted therapy. Although ICI-related myocarditis was successfully rescued with the wild-type CTLA-4–Ig, abatacept (14, 15), our data presented here demonstrate that it compromises the antitumor activity of ipilimumab. The CTLA-4 mutant fusion proteins belatacept and M17-2 ameliorated myocarditis and

other irAEs without interfering with the antitumor therapeutic effect. These findings provide an important basis for the clinical management of irAEs with soluble CTLA-4–Ig proteins.

Both abatacept and belatacept are recombinant fusion proteins comprising the extracellular domain of CTLA-4 and an IgFc region. Belatacept has missense mutations that differentiated it from abatacept, resulting in enhanced ability to disrupt CD28–B7-2-mediated costimulatory signals, which are thought to drive the initial alloreactive immune responses (35). Belatacept is currently approved for the prophylaxis of organ rejection in kidney transplantation (36, 37). Abatacept has been approved for the treatment of patients with rheumatoid arthritis (RA) (38, 39) and juvenile idiopathic arthritis (40, 41). In addition, abatacept has been reported to cure multiple autoimmune diseases (38, 42), including those with defective expression of CTLA-4 (13). Several preclinical studies have indicated the potential efficacy of abatacept for myocarditis (43, 44), and a clinical trial to evaluate the effects of abatacept on myocarditis in patients with RA is underway (ClinicalTrials.gov number NCT03619876). In this study, we found that abatacept, which binds to ipilimumab, completely impeded the therapeutic effect of ipilimumab; thus, our data raise the important concern as to the risk of using abatacept to treat irAEs in patients undergoing anti–CTLA-4 treatment. In contrast, belatacept ameliorated irAEs without impeding immunotherapy, making it an ideal drug for the management of irAEs in patients undergoing ICI treatment for cancer. Another mutant CTLA-4 protein, M17-2, had similar therapeutic activity against irAEs while preserving the immunotherapeutic effect of ICI.

Consistent with the essential role of CD28 signaling in T cell priming, we found that anti-B7 blockade compromised the antitumor efficacy of ipilimumab if it was delivered before tumor cell challenge, presumably because it has prevented the priming of tumor-reactive T cells. Nevertheless, belatacept and M17-2 did not affect the therapeutic effect of ipilimumab or anti–PD-1 in multiple established tumor models when they were delivered concurrently with immunotherapy or even after irAEs had occurred. Therefore, belatacept and M17-2 intervention have no detrimental effect on tumor rejection once tumor-reactive T cells have been primed.

Preclinical studies and one clinical case report have shown that abatacept could effectively rescue myocarditis caused by anti–PD-1 monotherapy or anti–CTLA-4 and anti–PD-1 combination therapy. However, it is not clear whether abatacept adversely affect antitumor efficacy. Here, we showed that abatacept affected the antitumor effect of ipilimumab by interfering with the binding between antibody and CTLA-4 in mice tumor models. Meanwhile, belatacept and M17-2 alleviated myocarditis, as well as clinically observable anemia and multiple organ inflammation, caused by ipilimumab + anti–PD-1 therapy but did not affect the antitumor efficacy. Our data indicate that soluble CTLA-4–Ig proteins would be effective unless an anti–CTLA-4 mAb and the fusion proteins are mutually neutralizing. Considering that ipilimumab or ipilimumab + anti–PD-1 therapy induces irAEs that are more severe than PD-1–targeted monotherapy, future clinical development for irAE therapy should focus on mutant CTLA-4–Ig proteins that bind to B7-1/B7-2 but not to the therapeutic anti–CTLA-4 antibodies. We further demonstrated that the mutant fusion proteins also protect irAE induced by recently approved tremelimumab in combination with anti–PD-1. Similar approaches can be used to identify suitable mutant fusion proteins by

their ability to avoid binding to therapeutic anti–CTLA-4 mAbs while retaining binding to B7-1 and B7-2. As expected, neither abatacept nor mutant CTLA-4 fusion proteins compromised anti–PD-1 monotherapy; thus all three proteins may be used for PD-1–based immunotherapy that does not involve concurrent anti–CTLA-4 treatment.

It is worth noting three limitations of the animal model used in this study. First, the animal model expresses hCTLA-4 but mouse B7-1, B7-2, and CD28. Because the fusion proteins bound mouse B7 less well than the human counterparts, it is possible that the fusion proteins may be more efficient in blocking the B7-1 and B7-2 interaction with CD28 in humans than in the mouse model. This concern is partially addressed using sufficient doses of fusion proteins to fully block the mouse B7-CD28 interaction in vivo, as demonstrated by potent inhibition of ADAs and by reduction of immune activation in the draining lymph nodes. Second, because adult mice were more resistant to irAE, very young mice were needed to elicit robust irAE to clearly demonstrate therapeutic effects (24). Future clinical studies will help to address whether the mouse model fully recapitulates pathogenesis of human irAE. Third, because of different manufacturing processes for M17 and belatacept, it is unclear whether the apparent difference in pharmacokinetics of two molecules is intrinsic to the molecular structures or related to production. The difference does not change the conclusion because we adjusted dosing on the basis of the pharmacokinetics to ensure comparable exposure.

Together, our data presented here demonstrate that soluble CTLA-4–Ig variants can be generated to ameliorate irAEs in multiple organs without compromising the antitumor effects of anti–CTLA-4 therapy. This may allow the opportunity to safely increase the dose of anti–CTLA-4 as a monotherapy and in combination therapy, further strengthening the antitumor efficacy. In contrast, the wild-type CTLA-4–Ig abatacept may weaken the immunotherapeutic effect of anti–CTLA-4 antibodies. Our data suggest a promising strategy to manage irAEs induced by CTLA-4– or PD-1–targeted therapy and thus unleash the full potential of CTLA-4–targeting immunotherapy.

MATERIALS AND METHODS

Study design

The aim of this study was to test whether irAEs can be overcome by provision of soluble CTLA-4 mutants without negatively affecting the antitumor effect of anti–CTLA-4 or anti–PD-1 mAbs. We performed systematic site-directed mutagenesis, engineered a series of CTLA-4–Ig mutants as candidates, and then screened their binding activity to B7-1/B7-2 and anti–CTLA-4 mAbs by enzyme-linked immunosorbent assays (ELISAs). Using multiple murine tumor models, we evaluated whether CTLA-4–Ig fusion protein compromises antitumor activity of ipilimumab or anti–PD-1 mAb. Using the *CTLA4*$^{h/h}$ mouse model, we evaluated the prophylactic and treatment effects of CTLA-4–Ig mutants on irAEs by CBC, histopathological analysis, and an ALT activity assay. Last, we explored the mechanism of the protective effect of belatacept against irAEs by flow cytometry. All animal studies were performed at the Research Animal Facility of Children's Research Institute at the Children's National Medical Center or the Institute of Human Virology at the University of Maryland School of Medicine. All studies have been approved by the Institutional Animal Care and

Use Committee. Sample sizes were calculated by the investigators on the basis of previous experience. The investigators were not blinded to allocation during experiments or analysis with the exception of histopathological score. All experiments were performed at least twice, and some data were combined from several independent experiments as described in the figure legends. No outlier values were excluded.

Experimental animals

C57BL/6 mice that express the CTLA-4 protein with 100% identity to hCTLA-4 protein under the control of the endogenous mouse *Ctla4* locus, *CTLA4*$^{h/h}$, have been previously described (45). Adult mice (6 to 10 weeks old) were used for tumor models, whereas young mice (10 days old) were used for irAE studies as previously reported (16, 24). All mice were maintained at the Research Animal Facility of Children's Research Institute at the Children's National Medical Center or the Institute of Human Virology at the University of Maryland Baltimore School of Medicine. All studies involving mice have been approved by the Institutional Animal Care and Use Committee.

Cell culture and treatment

Chinese hamster ovary (CHO) cells transfected with mouse or human B7-1 or B7-2 have been described previously (46, 47). CHO cells transfected with wild-type orange fluorescent protein (OFP)–hCTLA-4, OFP-hCTLA-Y201V, green fluorescent protein (GFP)–hB7-1, or GFP–hB7-2 have been described before (12, 24). The murine colon tumor cell line MC38 and melanoma cell line B16-F1 were purchased from the American Type Culture Collection. The EG7 cell line was a gift from C. Dong (Shanghai Immune Therapy Institute, Shanghai Jiao Tong University School of Medicine–Affiliated Renji Hospital). The EG7 cells were cultured in RPMI 1640 medium supplemented with 10% fetal bovine serum (FBS; HyClone), 2 mM L-glutamine, 0.05 mM 2-mercaptoethanol, penicillin (100 U/ml), and streptomycin (100 μg/ml; Gibco). Other cells were grown in Dulbecco's modified Eagle's medium (Gibco) supplemented with 10% FBS (HyClone), penicillin (100 U/ml), and streptomycin (100 μg/ml; Gibco). All cell lines were incubated at 37°C and were maintained in an atmosphere containing 5% CO_2.

Human peripheral blood mononuclear cells (PBMCs) were isolated by Ficoll density gradient centrifugation and were activated by the stimulation with anti-CD3 (2 μg/ml; OKT3, Invitrogen) and anti-CD28 (1 μg/ml; CD28.2, BioLegend) for 2 days. Surface CTLA-4 was analyzed by flow cytometry. Cells were cultured in RPMI 1640 medium (Gibco) supplemented with 10% FBS (HyClone), 2 mM L-glutamine, 0.05 mM 2-mercaptoethanol, penicillin (100 U/ml), and streptomycin (100 μg/ml; Gibco).

CTLA4$^{h/h}$ splenocytes were labeled with 2 μM carboxyfluorescein succinimidyl ester in phosphate-buffered saline (PBS) at 37°C for 10 min. Cells were washed three times with 10 volumes of complete RPMI 1640 medium. Splenocytes were then stimulated with anti-CD3 antibody in the presence of serial dilutions of CTLA-4–Ig or hIgFc for 3 days.

Antibodies and reagents

All mutant CTLA-4–Ig fusion proteins were generated by Sydlabs Inc. by transient expression in the 293 cell line. Clinical abatacept and belatacept were used for in vivo studies. Recombinant human and mouse (h/m)B7-1–Fc, h/mB7-2–Fc, and h/mCD28 were purchased from Sino Biological Inc. Recombinant ipilimumab with amino acid sequence disclosed in WC500109302 and www.drugbank.ca/drugs/DB06186 was provided by Lakepharma Inc. and Alphamab Inc. Clinical ipilimumab was also used for some of the studies. Recombinant Treme-IgG1 was produced by Sydlabs Inc. Mouse anti–PD-1 (RMP1-14), anti–mB7-1 (1G10), and anti–mB7-2 (GL1) mAbs were purchased from Bio X Cell Inc. Azide-free hIgGFc was purchased from Athens Research and Technology. Biotinylation was completed by conjugating EZ-Link Sulfo-NHS-LC-Biotin (Thermo Fisher Scientific) to desired proteins or cells according to the manufacturer's instructions.

Enzyme-linked immunosorbent assays

For CTLA-4–Ig and B7-1/B7-2/ipilimumab/Treme-IgG1 interaction assays, CTLA-4–Ig mutants (1 μg/ml) were precoated on 96-well high-binding polystyrene plates in PBS at 4°C overnight. After washing away the unbound protein, the plates were blocked with 1% bovine serum albumin (BSA) in PBS plus Tween 20 (PBST) and then incubated with a given concentration of biotinylated B7-1–Fc/B7-2–Fc/ipilimumab/Treme-IgG1 for 1.5 to 2 hours at room temperature. Plates were then washed five times with PBST and detected with horseradish peroxidase (HRP)–conjugated streptavidin. For the ADA assay, ipilimumab (2 μg/ml) was precoated on a plate in PBS at 4°C overnight. After washing away the unbound protein, the plates were blocked with 1% BSA in PBST and then incubated with series dilution of serum samples for 2 hours at room temperature. The plates were then washed with PBST five times and detected with HRP-conjugated anti-mIgG. Absorbance was measured by optical density at 450 nm (OD_{450}) of wavelength using a microplate reader (SpectraMax iD3, Molecular Devices).

Assays for B7–CTLA-4/CD28 interaction

To measure hCTLA-4 and hB7-1/B7-2 interactions, 1×10^5 hCTLA-4–Y201V–expressing cells were incubated with biotinylated hB7-1 or hB7-2 (1 μg/ml) in the presence of a given dose of CTLA-4–Ig or hIgFc at 4°C for 30 min. The amounts of bound receptors were measured using phycoerythrin (PE)–conjugated streptavidin. For hCD28 and hB7-1/B7-2 interaction, 1×10^5 hB7-1– or hB7-2–expressing CHO cells were incubated with biotinylated hCD28 (5 μg/ml) in the presence of a given dose of CTLA-4–Ig or hIgFc and detected by streptavidin-PE. For mCD28 and mB7-1/B7-2 interaction, 1×10^5 mB7-1– or mB7-2–expressing CHO cells were incubated with biotinylated mCD28 (10 μg/ml) in the presence of a given dose of CTLA-4–Ig or hIgFc and detected by streptavidin-PE. Flow cytometry was performed using FACSCanto II (BD Biosciences), and data were analyzed by Flowjo (Tree Star Inc.).

Trans-endocytosis assay

Plasmids with GFP-tagged (C-GFPSpark tag) hB7-2/B7-1 and OFP-tagged (C-OFPSpark tag) hCTLA-4 cDNA were purchased from Sino Biological Inc. and used to establish stable

CHO cell lines expressing either molecule. To measure inhibition of trans-endocytosis by CTLA-4–Ig fusion proteins, GFP-tagged B7-expressing CHO cells were cocultured with OFP-tagged CTLA-4–expressing CHO cells in the presence of given doses of CTLA-4–Ig fusion proteins at 37°C for 4 hours. The percentage of trans-endocytosis was calculated as $(GFP^+OFP^+\%) / (GFP^+OFP^+\% + GFP^-OFP^+\%) \times 100$.

irAE model and histopathological analysis

Young *CTLA4*$^{h/h}$ mice were treated intraperitoneally with ipilimumab and anti–PD-1 mAb at a dose of 100 μg per mouse per injection every 3 days for a total of four injections, starting on day 10 of birth. Belatacept (100 μg), M17-2 (300μg), or hIgFc (100 μg) treatment was initiated intraperitoneally simultaneously with ICI therapy or after ICI therapy completion for a total of three or four injections. To avoid cage variation, mice in the same cages were individually tagged and separated to different groups on the basis of body weight. Organs from mice that received therapeutics or control antibodies were harvested and fixed in formalin. Hematoxylin and eosin (H&E) staining was performed by Histoserv Inc. Inflammation status of those organs was scored double-blind. Score criteria have been described previously (24). Data shown are the scores for single organs or the combined scores of all organs examined.

Complete blood counts

Blood samples (50 μl) were collected through the submandibular vein using tubes with K2EDTA (BD Biosciences). Samples were analyzed by HEMAVET HV950 (Drew Scientific Group) or VETSCAN HM5 Hematology Analyzer (Zoetis). Analysis was conducted following the manufacturer's instructions.

Tumor models and treatment

MC38 (5×10^5 to 8×10^5), EG7 (1×10^6 to 2×10^6), or B16-F10 (1×10^5 to 2×10^5) was injected subcutaneously into the flanks of 6- to 10-week-old *CTLA4*$^{h/h}$ mice. Tumor volumes were measured by length (a) and width (b) and calculated as tumor volume = $ab^2/2$. Immunotherapies were initiated at 5 to 7 days after tumor inoculation with indicated doses. Mice with tumor volumes less than 2000 mm^3 were considered to be surviving. For long-term immune memory evaluation, mice underwent complete tumor regression after ipilimumab + hIgFc, belatacept, or M17-2 treatment was rechallenged with 4×10^6 MC38 cells (five times the primary tumor inoculation) after primary tumors had not been detected for more than 1 to 2 months. Naïve mice were injected with the same number tumor cells as controls.

Flow cytometry

Tumor tissues were minced into small pieces; digested with collagenase IV (1 mg/ml; catalog no. C5138, Sigma-Aldrich), hyaluronidase (0.1 mg/ml; catalog no. H6254, Sigma-Aldrich), and deoxyribonuclease I (0.01 mg/ml; catalog no. D5025, Sigma-Aldrich) for 30 min at 37°C; washed; and filtered through 100-μm cell strainers. Hearts and livers were minced into small pieces and digested with Liberase (0.26 U/ml; catalog no. 5401119001, Sigma-Aldrich) and deoxyribonuclease I (0.01 mg/ml) at 37°C for 30 min. Single-cell

suspensions were blocked with anti-FcR (clone 2.4G2, Bio X Cell) and then stained with antibodies for flow cytometry. For intracellular staining of IFN-γ, granzyme B, IL-4, and IL-17A, cells were stimulated with phorbol 12-myristate 13-acetate (PMA) and ionomycin (Sigma-Aldrich) together with brefeldin A (eBioscience) blockade for 4 hours. Blood samples (50 μl) were collected into tubes with K2EDTA (BD Biosciences) and lysed with ACK-lysing buffer (Gibco). Single-cell suspensions were incubated with anti–Fc receptor (10 μg/ml; clone 2.4G2, Bio X Cell) for 10 min in FACS staining buffer (2% FBS in PBS). Subsequently, cells were stained with specific antibodies for 30 min on ice in the dark against the following: hCD4: PE–cyanine 7 (Cy7) (clone OKT4, catalog no. 317414, BioLegend) and Foxp3-PE (clone 236A/E7, catalog no. 12-4777-42, eBioscience); hCD25: Pacific Blue (clone M-A251, catalog no. 356130, BioLegend), B220-PE-Cy7 (clone RA3-6B2, catalog no. 103222, BioLegend), CD11b-allophycocyanin (APC)–eFluor780 (clone M1/70, catalog no. 4700112-82, Invitrogen), mCD25-PE (clone 3C7, catalog no. 101904, BioLegend), mCD3-PE (clone 145-2C11, catalog no. 12-0031-83, Invitrogen), mCD4-APC-eFluor780 (clone GK1.5, catalog no. 47-0041-82, eBioscience), mCD4-PE (clone GK1.5, catalog no. 12-0041-83, Invitrogen), CD44-PE-Cy7 (clone IM7, catalog no. 103030, BioLegend), CD45–Brilliant Violet 510 (clone 30-F11, catalog no. 563891, BD Biosciences), mCD45-eFluor450 (clone 30-F11, catalog no. 48-0451-82, Invitrogen), CD62L-APC (clone MEL-14, catalog no. 104412, BioLegend), mCD8-PerCP-Cy5.5 (clone 53-6.7, catalog no. 100734, BioLegend), F4/80-PE (clone T45-2342, catalog no. 565410, BD Biosciences), Foxp3-eFluor450 (clone FJK-16s, catalog no. 48-5773-82, eBioscience), Gr-1-APC (clone RB6-8C5, catalog no. 17-5931-82, Invitrogen), granzyme B–fluorescein isothiocyanate (FITC) (clone NGZB, catalog no. 11-8898-82, eBioscience), IFN-γ–APC (clone XMG1.2, catalog no. 17-7311-82, eBioscience), IL-17A-eFluor450 (clone eBio17B7, catalog no. 48-7177-82, Invitrogen), Ly6C-FITC (clone HK1.4, catalog no. 128006, BioLegend), NK1.1–PE-Cy7 (clone PK136, catalog no. 25-5941-82, Invitrogen), PD-1–APC (clone J43, catalog no. 17-9985-82, Invitrogen), and Tim-3–PE-Cy7 (clone RMT3-23, catalog no. 25-5870-82, Invitrogen). Intracellular staining was performed with the Intracellular Fixation and Permeabilization Kit (catalog no. 88-8824, eBioscience) according to the manufacturer's instructions. Live/dead cells were stained with the LIVE/DEAD Fixable Aqua Dead Cell Stain Kit (catalog no. L34957, Invitrogen) after cell surface staining. The dye was dissolved with 50 μl of dimethyl sulfoxide and diluted at 1:500 in PBS for staining. The samples were analyzed by a BD Canto II or LSR II flow cytometer, and data were analyzed by Flowjo software.

Statistical analysis

Raw, individual-level data for experiments where $n < 20$ are presented in data file S1. Mice were assigned at random to treatment groups for all mouse studies and, where possible, mixed among cages. Mice numbers (n) are stated in each figure legend. No mice were excluded from experiments unless indicated. Blinded staining and blinded analysis were performed for histopathological studies. Experiments were independently repeated two or three times. The specific tests used to analyze each set of experiments are indicated in the figure legends. Data were analyzed using a Mann-Whitney test to compare between two groups, either one-way ANOVA (analysis of variance) for multiple comparisons or two-way repeated-measures ANOVA for behavioral tests. To perform a cohort-based analysis

on the overall survival rate, the prognostic value of discrete variables was estimated using the Kaplan-Meier survival curves, and the log-rank test was used to estimate the significance among different survival curves. In the graphs, y-axis error bars represent the SEM as indicated. Statistical calculations were performed using GraphPad Prism software (GraphPad Software). Nonsignificant, $P > 0.05$; $*P < 0.05$; $**P < 0.01$; $***P < 0.001$.

Supplementary Material

Refer to Web version on PubMed Central for supplementary material.

Acknowledgments:

We thank members of Liu and Zheng Laboratories for discussion and support. Parts of the studies were performed while some of the co-authors were at the Children's National Medical Center in Washington, D.C.

Funding:

This study is supported by grants from the National Institutes of Health R01AI154722 to L.S., R01AI064350 to Y.L., National Cancer Institute R01CA227671 and R44CA250889 to P.Zheng,and Melanoma Research Alliance Award 559400 and an OncoC4 research agreement to M.L.

Data and materials availability:

All data associated with this study are present in the paper or the Supplementary Materials. Reagents used in this work can be requested from Y.L. (yangl@oncoc4.com) and will be shared with the scientific community for research purpose via a material transfer agreement.

REFERENCES AND NOTES

1. Wolchok JD, Rollin L, Larkin J, Nivolumab and ipilimumab in advanced melanoma. N. Engl. J. Med 377, 2503–2504 (2017).
2. Motzer RJ, Tannir NM, McDermott DF, Frontera OA, Melichar B, Choueiri TK, Plimack ER, Barthelemy P, Porta C, George S, Powles T, Donskov F, Neiman V, Kollmannsberger CK, Salman P, Gurney H, Hawkins R, Ravaud A, Grimm MO, Bracarda S, Barrios CH, Tomita Y, Castellano D, Rini BI, Chen AC, Mekan S, McHenry MB, Wind-Rotolo M, Doan J, Sharma P, Hammers HJ, Escudier B; CheckMate 214 Investigators, Nivolumab plus ipilimumab versus sunitinib in advanced renal-cell carcinoma. N. Engl. J. Med 378, 1277–1290 (2018). [PubMed: 29562145]
3. Hellmann MD, Ciuleanu TE, Pluzanski A, Lee JS, Otterson GA, Audigier-Valette C, Minenza E, Linardou H, Burgers S, Salman P, Borghaei H, Ramalingam SS, Brahmer J, Reck M, O'Byrne KJ, Geese WJ, Green G, Chang H, Szustakowski J, Bhagavatheeswaran P, Healey D, Fu Y, Nathan F, Paz-Ares L, Nivolumab plus ipilimumab in lung cancer with a high tumor mutational burden. N. Engl. J. Med 378, 2093–2104 (2018). [PubMed: 29658845]
4. Wolchok JD, Kluger H, Callahan MK, Postow MA, Rizvi NA, Lesokhin AM, Segal NH, Ariyan CE, Gordon RA, Reed K, Burke MM, Caldwell A, Kronenberg SA, Agunwamba BU, Zhang X, Lowy I, Inzunza HD, Feely W, Horak CE, Hong Q, Korman AJ, Wigginton JM, Gupta A, Sznol M, Nivolumab plus ipilimumab in advanced melanoma. N. Engl. J. Med 369, 122–133 (2013). [PubMed: 23724867]
5. Larkin J, Hodi FS, Wolchok JD, Combined nivolumab and ipilimumab or monotherapy in untreated melanoma. N. Engl. J. Med 373, 1270–1271(2015).
6. Wolchok JD, Chiarion-Sileni V, Gonzalez R, Rutkowski P, Grob JJ, Cowey CL, Lao CD, Wagstaff J, Schadendorf D, Ferrucci PF, Smylie M, Dummer R, Hill A, Hogg D, Haanen J, Carlino MS, Bechter O, Maio M, Marquez-Rodas I, Guidoboni M, McArthur G, Lebbe C, Ascierto PA, Long GV, Cebon J, Sosman J, Postow MA, Callahan MK, Walker D, Rollin L, Bhore R, Hodi FS, Larkin

J, Overall survival with combined nivolumab and ipilimumab in advanced melanoma. N. Engl. J. Med 377, 1345–1356 (2017). [PubMed: 28889792]

7. Larkin J, Chiarion-Sileni V, Gonzalez R, Grob JJ, Rutkowski P, Lao CD, Cowey CL, Schadendorf D, Wagstaff J, Dummer R, Ferrucci PF, Smylie M, Hogg D, Hill A, Marquez-Rodas I, Haanen J, Guidoboni M, Maio M, Schoffski P, Carlino MS, Lebbe C, McArthur G, Ascierto PA, Daniels GA, Long GV, Bastholt L, Rizzo JI, Balogh A, Moshyk A, Hodi FS, Wolchok JD, Five-year survival with combined nivolumab and ipilimumab in advanced melanoma. N. Engl. J. Med 381, 1535–1546 (2019). [PubMed: 31562797]
8. Amaria RN, Reddy SM, Tawbi HA, Davies MA, Ross MI, Glitza IC, Cormier JN, Lewis C, Hwu WJ, Hanna E, Diab A, Wong MK, Royal R, Gross N, Weber R, Lai SY, Ehlers R, Blando J, Milton DR, Woodman S, Kageyama R, Wells DK, Hwu P, Patel SP, Lucci A, Hessel A, Lee JE, Gershenwald J, Simpson L, Burton EM, Posada L, Haydu L, Wang L, Zhang S, Lazar AJ, Hudgens CW, Gopalakrishnan V, Reuben A, Andrews MC, Spencer CN, Prieto V, Sharma P, Allison J, Tetzlaff MT, Wargo JA, Neoadjuvant immune checkpoint blockade in high-risk resectable melanoma. Nat. Med 24, 1649–1654 (2018). [PubMed: 30297909]
9. Blank CU, Rozeman EA, Fanchi LF, Sikorska K, van de Wiel B, Kvistborg P, Krijgsman O, van den Braber M, Philips D, Broeks A, van Thienen JV, Mallo HA, Adriaansz S, Ter Meulen S, Pronk LM, Grijpink-Ongering LG, Bruining A, Gittelman RM, Warren S, van Tinteren H, Peeper DS, Haanen J, van Akkooi ACJ, Schumacher TN, Neoadjuvant versus adjuvant ipilimumab plus nivolumab in macroscopic stage III melanoma. Nat. Med 24, 1655–1661 (2018). [PubMed: 30297911]
10. Wang DY, Salem JE, Cohen JV, Chandra S, Menzer C, Ye F, Zhao S, Das S, Beckermann KE, Ha L, Rathmell WK, Ancell KK, Balko JM, Bowman C, Davis EJ, Chism DD, Horn L, Long GV, Carlino MS, Lebrun-Vignes B, Eroglu Z, Hassel JC, Menzies AM, Sosman JA, Sullivan RJ, Moslehi JJ, Johnson DB, Fatal toxic effects associated with immune checkpoint inhibitors: A systematic review and meta-analysis. JAMA Oncol. 4, 1721–1728 (2018). [PubMed: 30242316]
11. Feng Y, Roy A, Masson E, Chen TT, Humphrey R, Weber JS, Exposure-response relationships of the efficacy and safety of ipilimumab in patients with advanced melanoma. Clin. Cancer Res 19, 3977–3986 (2013). [PubMed: 23741070]
12. Zhang Y, Du X, Liu M, Tang F, Zhang P, Ai C, Fields JK, Sundberg EJ, Latinovic OS, Devenport M, Zheng P, Liu Y, Hijacking antibody-induced CTLA-4 lysosomal degradation for safer and more effective cancer immunotherapy. Cell Res. 29, 609–627 (2019). [PubMed: 31267017]
13. Lo B, Zhang K, Lu W, Zheng L, Zhang Q, Kanellopoulou C, Zhang Y, Liu Z, Fritz JM, Marsh R, Husami A, Kissell D, Nortman S, Chaturvedi V, Haines H, Young LR, Mo J, Filipovich AH, Bleesing JJ, Mustillo P, Stephens M, Rueda CM, Chougnet CA, Hoebe K, McElwee J, Hughes JD, Karakoc-Aydiner E, Matthews HF, Price S, Su HC, Rao VK, Lenardo MJ, Jordan MB, Patients with LRBA deficiency show CTLA4 loss and immune dysregulation responsive to abatacept therapy. Science 349, 436–440 (2015). [PubMed: 26206937]
14. Wei SC, Meijers WC, Axelrod ML, Anang NAS, Screever EM, Wescott EC, Johnson DB, Whitley E, Lehmann L, Courand PY, Mancuso JJ, Himmel LE, Lebrun-Vignes B, Wleklinski MJ, Knollmann BC, Srinivasan J, Li Y, Atolagbe OT, Rao X, Zhao Y, Wang J, Ehrlich LIR, Sharma P, Salem JE, Balko JM, Moslehi JJ, Allison JP, A genetic mouse model recapitulates immune checkpoint inhibitor-associated myocarditis and supports a mechanism-based therapeutic intervention. Cancer Discov. 11, 614–625 (2021). [PubMed: 33257470]
15. Salem JE, Allenbach Y, Vozy A, Brechot N, Johnson DB, Moslehi JJ, Kerneis M, Abatacept for severe immune checkpoint inhibitor-associated myocarditis. N. Engl. J. Med 380, 2377–2379 (2019). [PubMed: 31189043]
16. Du X, Tang F, Liu M, Su J, Zhang Y, Wu W, Devenport M, Lazarski CA, Zhang P, Wang X, Ye P, Wang C, Hwang E, Zhu T, Xu T, Zheng P, Liu Y, A reappraisal of CTLA-4 checkpoint blockade in cancer immunotherapy. Cell Res. 28, 416–432 (2018). [PubMed: 29472691]
17. Selby MJ, Engelhardt JJ, Quigley M, Henning KA, Chen T, Srinivasan M, Korman AJ, Anti-CTLA-4 antibodies of IgG2a isotype enhance antitumor activity through reduction of intratumoral regulatory T cells. Cancer Immunol. Res 1, 32–42 (2013). [PubMed: 24777248]
18. Simpson TR, Li F, Montalvo-Ortiz W, Sepulveda MA, Bergerhoff K, Arce F, Roddie C, Henry JY, Yagita H, Wolchok JD, Peggs KS, Ravetch JV, Allison JP, Quezada SA, Fc-dependent depletion

of tumor-infiltrating regulatory T cells co-defines the efficacy of anti-CTLA-4 therapy against melanoma. J. Exp. Med 210, 1695–1710 (2013). [PubMed: 23897981]

19. Bulliard Y, Jolicoeur R, Windman M, Rue SM, Ettenberg S, Knee DA, Wilson NS, Dranoff G, Brogdon JL, Activating Fc γ receptors contribute to the antitumor activities of immunoregulatory receptor-targeting antibodies. J. Exp. Med 210, 1685–1693 (2013). [PubMed: 23897982]
20. Linsley PS, Wallace PM, Johnson J, Gibson MG, Greene JL, Ledbetter JA, Singh C, Tepper MA, Immunosuppression in vivo by a soluble form of the CTLA-4 T cell activation molecule. Science 257, 792–795 (1992). [PubMed: 1496399]
21. Liu Y, Jones B, Brady W, Janeway CA Jr., Linsley PS, Co-stimulation of murine CD4 T cell growth: Cooperation between B7 and heat-stable antigen. Eur. J. Immunol 22, 2855–2859 (1992). [PubMed: 1385153]
22. Larkin J, Chiarion-Sileni V, Gonzalez R, Grob JJ, Cowey CL, Lao CD, Schadendorf D, Dummer R, Smylie M, Rutkowski P, Ferrucci PF, Hill A, Wagstaff J, Carlino MS, Haanen JB, Maio M, Marquez-Rodas I, McArthur GA, Ascierto PA, Long GV, Callahan MK, Postow MA, Grossmann K, Sznol M, Dreno B, Bastholt L, Yang A, Rollin LM, Horak C, Hodi FS, Wolchok JD, Combined nivolumab and ipilimumab or monotherapy in untreated melanoma. N. Engl. J. Med 373, 23–34 (2015). [PubMed: 26027431]
23. Hellmann MD, Rizvi NA, Goldman JW, Gettinger SN, Borghaei H, Brahmer JR, Ready NE, Gerber DE, Chow LQ, Juergens RA, Shepherd FA, Laurie SA, Geese WJ, Agrawal S, Young TC, Li X, Antonia SJ, Nivolumab plus ipilimumab as first-line treatment for advanced non-small-cell lung cancer (CheckMate 012): Results of an open-label, phase 1, multicohort study. Lancet Oncol. 18, 31–41 (2017). [PubMed: 27932067]
24. Du X, Liu M, Su J, Zhang P, Tang F, Ye P, Devenport M, Wang X, Zhang Y, Liu Y, Zheng P, Uncoupling therapeutic from immunotherapy-related adverse effects for safer and effective anti-CTLA-4 antibodies in CTLA4 humanized mice. Cell Res. 28, 433–447 (2018). [PubMed: 29463898]
25. Borriello F, Sethna MP, Boyd SD, Schweitzer AN, Tivol EA, Jacoby D, Strom TB, Simpson EM, Freeman GJ, Sharpe AH, B7-1 and B7-2 have overlapping, critical roles in immunoglobulin class switching and germinal center formation. Immunity 6, 303–313 (1997). [PubMed: 9075931]
26. Johnson DB, Balko JM, Compton ML, Chalkias S, Gorham J, Xu Y, Hicks M, Puzanov I, Alexander MR, Bloomer TL, Becker JR, Slosky DA, Phillips EJ, Pilkinton MA, Craig-Owens L, Kola N, Plautz G, Reshef DS, Deutsch JS, Deering RP, Olenchock BA, Lichtman AH, Roden DM, Seidman CE, Koralnik IJ, Seidman JG, Hoffman RD, Taube JM, Diaz LA Jr., Anders RA, Sosman JA, Moslehi JJ, Fulminant myocarditis with combination immune checkpoint blockade. N. Engl. J. Med 375, 1749–1755 (2016). [PubMed: 27806233]
27. Heinzerling L, Ott PA, Hodi FS, Husain AN, Tajmir-Riahi A, Tawbi H, Pauschinger M, Gajewski TF, Lipson EJ, Luke JJ, Cardiotoxicity associated with CTLA4 and PD1 blocking immunotherapy. J. Immunother. Cancer 4, 50 (2016). [PubMed: 27532025]
28. Escudier M, Cautela J, Malissen N, Ancedy Y, Orabona M, Pinto J, Monestier S, Grob JJ, Scemama U, Jacquier A, Lalevee N, Barraud J, Peyrol M, Laine M, Bonello L, Paganelli F, Cohen A, Barlesi F, Ederhy S, Thuny F, Clinical features, management, and outcomes of immune checkpoint inhibitor-related cardiotoxicity. Circulation 136, 2085–2087 (2017). [PubMed: 29158217]
29. Moslehi JJ, Salem JE, Sosman JA, Lebrun-Vignes B, Johnson DB, Increased reporting of fatal immune checkpoint inhibitor-associated myocarditis. Lancet 391, 933 (2018).
30. Sanmamed MF, Chen L, A paradigm shift in cancer immunotherapy: From enhancement to normalization. Cell 175, 313–326 (2018). [PubMed: 30290139]
31. Liu Y, Zheng P, Preserving the CTLA-4 checkpoint for safer and more effective cancer immunotherapy. Trends Pharmacol. Sci 41, 4–12 (2020). [PubMed: 31836191]
32. de Coana YP, Wolodarski M, Poschke I, Yoshimoto Y, Yang Y, Nystrom M, Edback U, Brage SE, Lundqvist A, Masucci GV, Hansson J, Kiessling R, Ipilimumab treatment decreases monocytic MDSCs and increases CD8 effector memory T cells in long-term survivors with advanced melanoma. Oncotarget 8, 21539–21553 (2017). [PubMed: 28423487]

33. May KF Jr., Chang X, Zhang H, Lute KD, Zhou P, Kocak E, Zheng P, Liu Y, B7-deficient autoreactive T cells are highly susceptible to suppression by CD4(+)CD25(+) regulatory T cells. J. Immunol 178, 1542–1552 (2007). [PubMed: 17237403]
34. Zhou P, Zheng X, Zhang H, Liu Y, Zheng P, B7 blockade alters the balance between regulatory T cells and tumor-reactive T cells for immunotherapy of cancer. Clin. Cancer Res 15, 960–970 (2009). [PubMed: 19188167]
35. Larsen CP, Pearson TC, Adams AB, Tso P, Shirasugi N, Strobert E, Anderson D, Cowan S, Price K, Naemura J, Emswiler J, Greene J, Turk LA, Bajorath J, Townsend R, Hagerty D, Linsley PS, Peach RJ, Rational development of LEA29Y (belatacept), a high-affinity variant of CTLA4-Ig with potent immunosuppressive properties. Am. J. Transplant 5, 443–453 (2005). [PubMed: 15707398]
36. Dharnidharka VR, Costimulation blockade with belatacept in renal transplantation. N. Engl. J. Med 353, 2085–2086 (2005). [PubMed: 16282187]
37. Vincenti F, Larsen C, Durrbach A, Wekerle T, Nashan B, Blancho G, Lang P, Grinyo J, Halloran PF, Solez K, Hagerty D, Levy E, Zhou W, Natarajan K, Charpentier B, G. Belatacept Study, Costimulation blockade with belatacept in renal transplantation. N. Engl. J. Med 353, 770–781 (2005). [PubMed: 16120857]
38. Kremer JM, Westhovens R, Leon M, Di Giorgio E, Alten R, Steinfeld S, Russell A, Dougados M, Emery P, Nuamah IF, Williams GR, Becker JC, Hagerty DT, Moreland LW, Treatment of rheumatoid arthritis by selective inhibition of T-cell activation with fusion protein CTLA4Ig. N. Engl. J. Med 349, 1907–1915 (2003). [PubMed: 14614165]
39. Kremer JM, Dougados M, Emery P, Durez P, Sibilia J, Shergy W, Steinfeld S, Tindall E, Becker JC, Li T, Nuamah IF, Aranda R, Moreland LW, Treatment of rheumatoid arthritis with the selective costimulation modulator abatacept: Twelve-month results of a phase iib, double-blind, randomized, placebo-controlled trial. Arthritis Rheum. 52, 2263–2271 (2005). [PubMed: 16052582]
40. Ruperto N, Lovell DJ, Quartier P, Paz E, Rubio-Perez N, Silva CA, Abud-Mendoza C, Burgos-Vargas R, Gerloni V, Melo-Gomes JA, Saad-Magalhaes C, Sztajnbok F, Goldenstein-Schainberg C, Scheinberg M, Penades IC, Fischbach M, Orozco J, Hashkes PJ, Hom C, Jung L, Lepore L, Oliveira S, Wallace CA, Sigal LH, Block AJ, Covucci A, Martini A, Giannini EH; Paediatric Rheumatology INternational Trials Organization; Pediatric Rheumatology Collaborative Study Group, Abatacept in children with juvenile idiopathic arthritis: A randomised, double-blind, placebo-controlled withdrawal trial. Lancet 372, 383–391 (2008). [PubMed: 18632147]
41. Ruperto N, Lovell DJ, Quartier P, Paz E, Rubio-Perez N, Silva CA, Abud-Mendoza C, Burgos-Vargas R, Gerloni V, Melo-Gomes JA, Saad-Magalhaes C, Chavez-Corrales J, Huemer C, Kivitz A, Blanco FJ, Foeldvari I, Hofer M, Horneff G, Huppertz HI, Job-Deslandre C, Loy A, Minden K, Punaro M, Nunez AF, Sigal LH, Block AJ, Nys M, Martini A, Giannini EH; Paediatric Rheumatology International Trials Organization and the Pediatric Rheumatology Collaborative Study Group, Long-term safety and efficacy of abatacept in children with juvenile idiopathic arthritis. Arthritis Rheum 62, 1792–1802 (2010). [PubMed: 20191582]
42. Abrams JR, Lebwohl MG, Guzzo CA, Jegasothy BV, Goldfarb MT, Goffe BS, Menter A, Lowe NJ, Krueger G, Brown MJ, Weiner RS, Birkhofer MJ, Warner GL, Berry KK, Linsley PS, Krueger JG, Ochs HD, Kelley SL, Kang S, CTLA4Ig-mediated blockade of T-cell costimulation in patients with psoriasis vulgaris. J. Clin. Invest 103, 1243–1252 (1999). [PubMed: 10225967]
43. Kallikourdis M, Martini E, Carullo P, Sardi C, Roselli G, Greco CM, Vignali D, Riva F, Ormbostad Berre AM, Stolen TO, Fumero A, Faggian G, Di Pasquale E, Elia L, Rumio C, Catalucci D, Papait R, Condorelli G, T cell costimulation blockade blunts pressure overload-induced heart failure. Nat. Commun 8, 14680 (2017). [PubMed: 28262700]
44. Martini E, Cremonesi M, Panico C, Carullo P, Bonfiglio CA, Serio S, Jachetti E, Colombo MP, Condorelli G, Kallikourdis M, T cell costimulation blockade blunts age-related heart failure. Circ. Res 127, 1115–1117 (2020). [PubMed: 32806992]
45. Lute KD, May KF Jr., Lu P, Zhang H, Kocak E, Mosinger B, Wolford C, Phillips G, Caligiuri MA, Zheng P, Liu Y, Human CTLA4 knock-in mice unravel the quantitative link between tumor immunity and autoimmunity induced by anti-CTLA-4 antibodies. Blood 106, 3127–3133 (2005). [PubMed: 16037385]

46. Wu Y, Guo Y, Huang A, Zheng P, Liu Y, CTLA-4-B7 interaction is sufficient to costimulate T cell clonal expansion. J. Exp. Med 185, 1327–1336 (1997). [PubMed: 9104819]

47. Wu Y, Guo Y, Liu Y, A major costimulatory molecule on antigen-presenting cells, CTLA4 ligand A, is distinct from B7. J. Exp. Med 178, 1789–1793 (1993). [PubMed: 8228824]

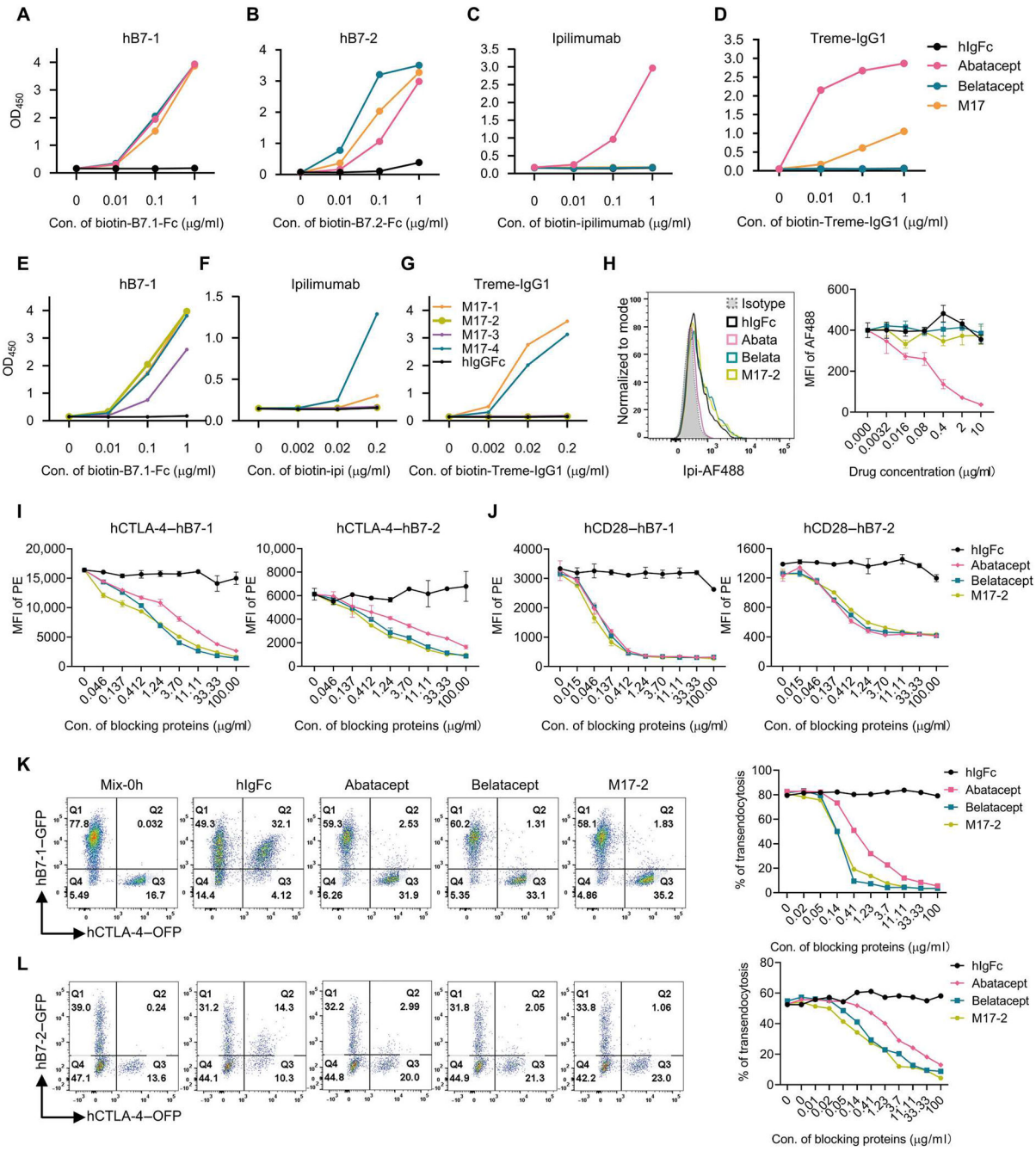

Fig. 1. A subset of CTLA-4 mutant fusion proteins bind to B7, but not to anti–CTLA-4, mAbs.

(**A** to **D**) Data shown are OD_{450} values from an ELISA using plates coated with indicated CTLA-4–Ig fusion proteins (1 μg/ml) and detected with the given concentration (Con.; 0 to 100 μg/ml) of biotinylated hB7-1Fc (A), hB7-2Fc (B), ipilimumab (C) or Treme-IgG1 (D). (**E** to **G**) Data shown are OD_{450} values from an ELISA using plates coated with indicated M17 mutations (1 μg/ml) and detected by the given concentration of biotinylated hB7-1Fc (E), ipilimumab (F), or Treme-IgG1 (G). (**H**) Anti-CD3/CD28 mAb-activated human PBMCs were incubated with Alexa Fluor 488 (AF488)–conjugated ipilimumab in

the presence of the given dose of CTLA-4–Ig or hIgFc. Representative flow cytometry histograms (fusion protein at 10 μg/ml; left) and quantitative mean fluorescence intensity (MFI) of AF488 (right) are shown. (**I**) hCTLA-4–Y201V–expressing cells were incubated with biotinylated hB7-1 or hB7-2 in the presence of the given dose of CTLA-4–Ig or hIgFc and detected by streptavidin-PE. (**J**) hB7-1–or hB7-2–expressing CHO cells were incubated with biotinylated hCD28 in the presence of the given dose of CTLA-4-Ig or hIgFc and detected by streptavidin-PE. (**K** and **L**) The ability of CTLA-4–Ig to block B7 trans-endocytosis by CTLA-4 was measured. CHO cells transfected with hCTLA-4–OFP and hB7-1–GFP (K) or B7-2–GFP (L) were cocultured in the presence of serial dilutions of CTLA-4–Ig or hIgFc for 4 hours at 37°C. Representative flow cytometry plots (left) and percentage of trans-endocytosis (right) are shown. Data are representative of at least two independent experiments.

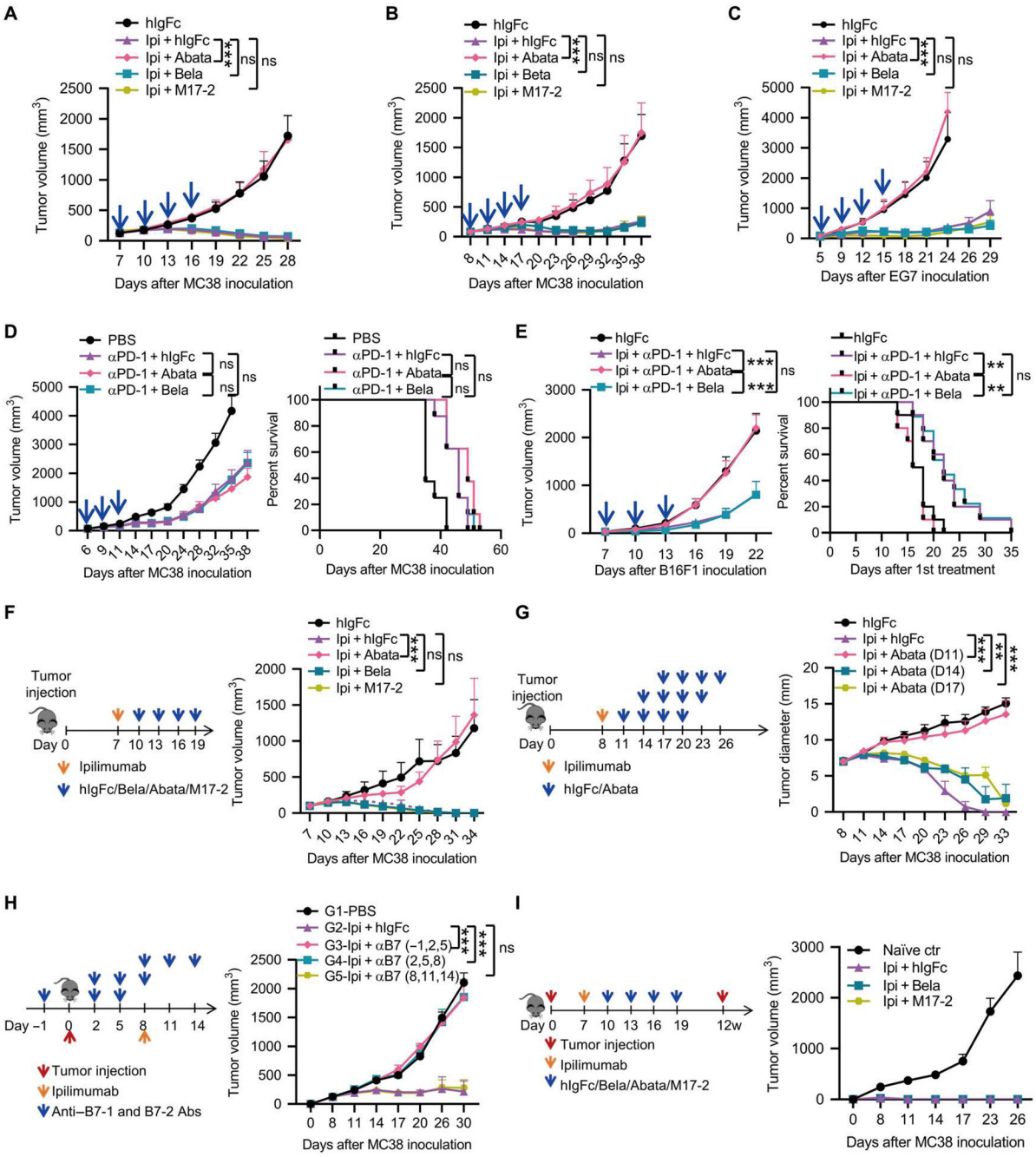

Fig. 2. CTLA-4 mutants preserve the therapeutic effects of ipilimumab treatment.

(**A**) Six- to 10-week-old MC38-bearing *CTLA4*$^{h/h}$ mice (n = 5 to 11) were treated intraperitoneally with 100 μg of ipilimumab and 100 μg of hIgFc, abatacept (Abata), or belatacept (Bela) or plus 300 μg of M17-2 on days 7, 10, 13, and 16. (**B**) Six- to 10-week-old MC38-bearing *CTLA4*$^{h/h}$ mice (n = 6) were treated intraperitoneally with 10 μg of ipilimumab and 100 μg of hIgFc, abatacept, or belatacept or plus 300 μg of M17-2 on days 8, 11, 14, and 17. (**C**) Six- to 10-week-old EG7-bearing *CTLA4*$^{h/h}$ mice (n = 5 to 10) were treated intraperitoneally with 100 μg of ipilimumab plus 100 μg of abatacept,

belatacept, or hIgFc or plus 300 μg of M17-2 on days 5, 9, 12, and 15. Tumor volumes are shown for (A) to (C). (**D**) Six- to 10-week-old MC38-bearing *CTLA4*$^{h/h}$ mice (n = 8) were treated intraperitoneally with 200 μg of anti–PD-1 (αPD-1) mAb (RMP1-14) plus 100 μg of abatacept, belatacept, or hIgFc on days 6, 9, and 11. Tumor volumes (left) and survival curves (right) are shown. (**E**) Six- to 10-week-old B16-bearing *CTLA4*$^{h/h}$ mice (n = 10) were treated intraperitoneally with 100 μg of ipilimumab plus 100 μg of anti–PD-1 (RMP1-14) together with 100 μg of abatacept, belatacept, or hIgFc on days 7, 10, and 13. Tumor volumes (left) and survival curves (right) are shown. (**F**) Six- to 10-week-old MC38-bearing *CTLA4*$^{h/h}$ mice (n = 5) were treated intraperitoneally with 100 μg of ipilimumab on day 7 and 100 μg of hIgFc, abatacept, or belatacept or plus 300 μg of M17-2 on days 10, 13, 16, and 19. Timeline of drug treatment (left) and tumor growth curves (right) are shown. (**G**) Six- to 10-week-old MC38-bearing *CTLA4*$^{h/h}$ mice (n = 6) were intraperitoneally treated with 100 μg of ipilimumab on day 7 and then treated with four injections of 100 μg of abatacept, respectively, starting on day 11, 14, or 17, every 3 days. Timeline of drug treatment (left) and tumor growth curves (right) are shown. (**H**) Six- to 10-week-old *CTLA4*$^{h/h}$ mice (n = 6) were subcutaneously inoculated with MC38 tumors on day 0. Anti–B7-1 (1G10) and anti–B7-2 (GL1) (αB7) mAbs were injected on indicated days at the dose of 300 μg for each mAb. Timeline of drug treatment (left) and tumor growth curves (right) are shown. (**I**) Mice previously cured of MC38 tumors [shown in (A)] or naïve mice (n = 4 or 5) were rechallenged subcutaneously with 4×10^6 MC38 cells on the opposite side from the primary tumors 2 months after complete rejection of primary tumors. Timeline of drug treatment (left) and tumor growth curves (right) are shown. Tumor growth curves were analyzed by two-way repeated-measures ANOVA with Bonferroni's multiple comparisons test. Survival curves were evaluated using Kaplan-Meier survival analyses. Statistical significance of the P value was determined by log-rank test. Data shown are means ± SEM. ns, $P \geq 0.05$, $^{**}P < 0.01$, and $^{***}P < 0.001$. Representative data of two or three independent experiments are shown.

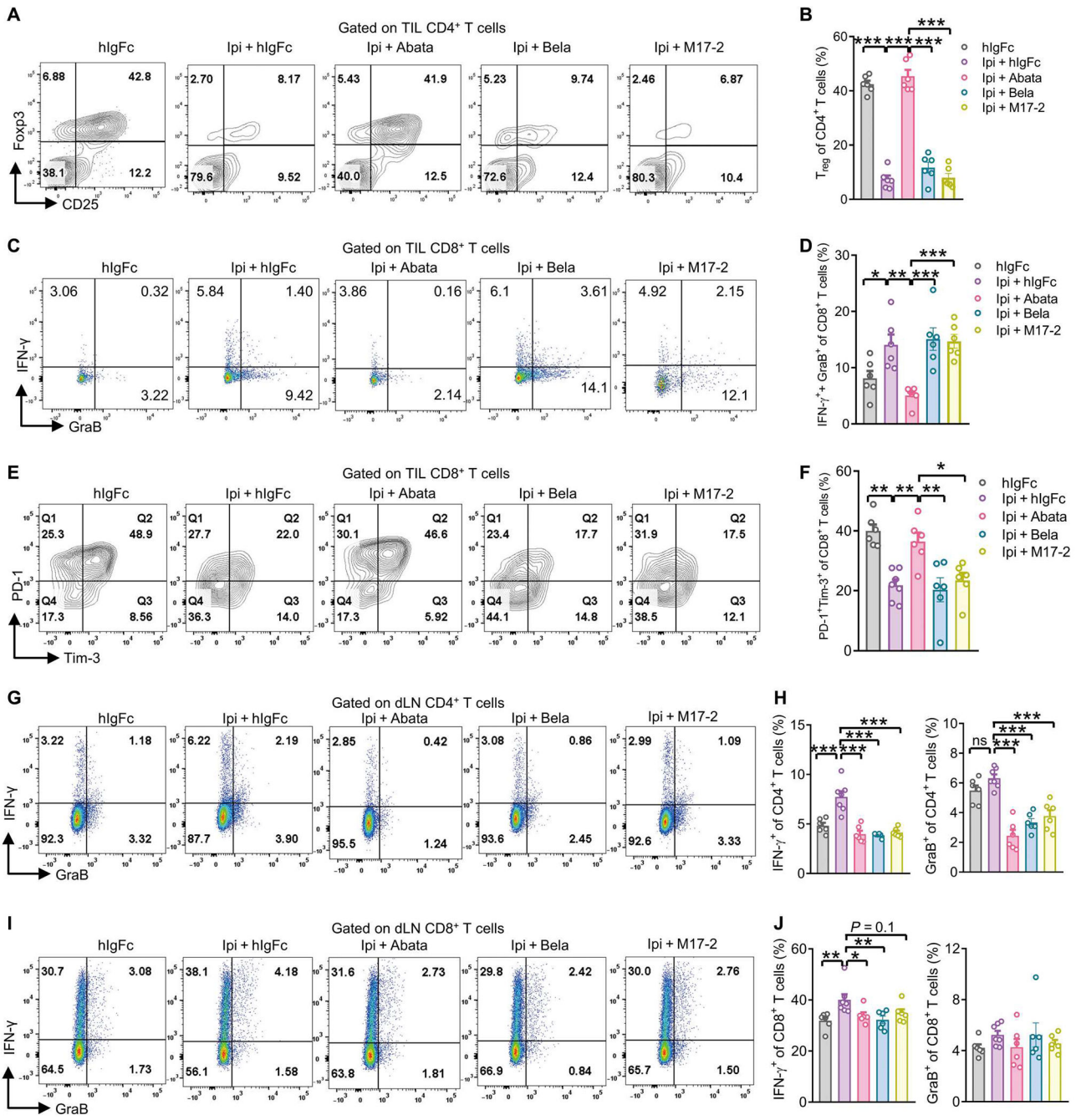

Fig. 3. CTLA-4 mutants abrogate T cell activation in draining lymph nodes, but not in the tumor microenvironment.

Six- to 10-week-old MC38-bearing-*CTLA4*$^{h/h}$ mice (n = 6 or 7) were treated intraperitoneally with 100 μg of ipilimumab plus 100 μg of hIgFc, abatacept, or belatacept or plus 300 μg of M17-2 on days 10, 13, and 16. Tumor masses and draining lymph nodes were collected on days 18 or 19 for flow cytometry analysis. (**A** and **B**) T_{reg} frequency among $CD4^+$ T cells in the tumor microenvironment was evaluated by flow cytometry. Representative flow cytometry profiles (A) and summary data (B) are shown. TIL, tumor-

infiltrating lymphocytes. (**C** and **D**) Shown is intracellular staining of tumor-infiltrating $CD8^+$ T cells for IFN-γ and granzyme B (GraB). Representative flow cytometry profiles (C) and summary data (D) are shown. (**E** and **F**) PD-1 and Tim-3 expression was measured on TIL $CD8^+$ T cells. Representative flow cytometry profiles (E) and summary data (F) are shown. (**G** to **J**) Shown is intracellular staining for IFN-γ and granzyme B in $CD4^+$ (G and H) and $CD8^+$ (I and J) T cells isolated from draining lymph nodes (dLNs). Representative flow cytometry profiles (G and I) and summary data (H and J) are shown. Data were analyzed by one-way ANOVA with Bonferroni's correction for multiple comparisons. Data presented are means ± SEM. ns, $P \geq 0.05$; $^*P < 0.05$; $^{**}P < 0.01$; $^{***}P < 0.001$. Representative data of two independent experiments are shown.

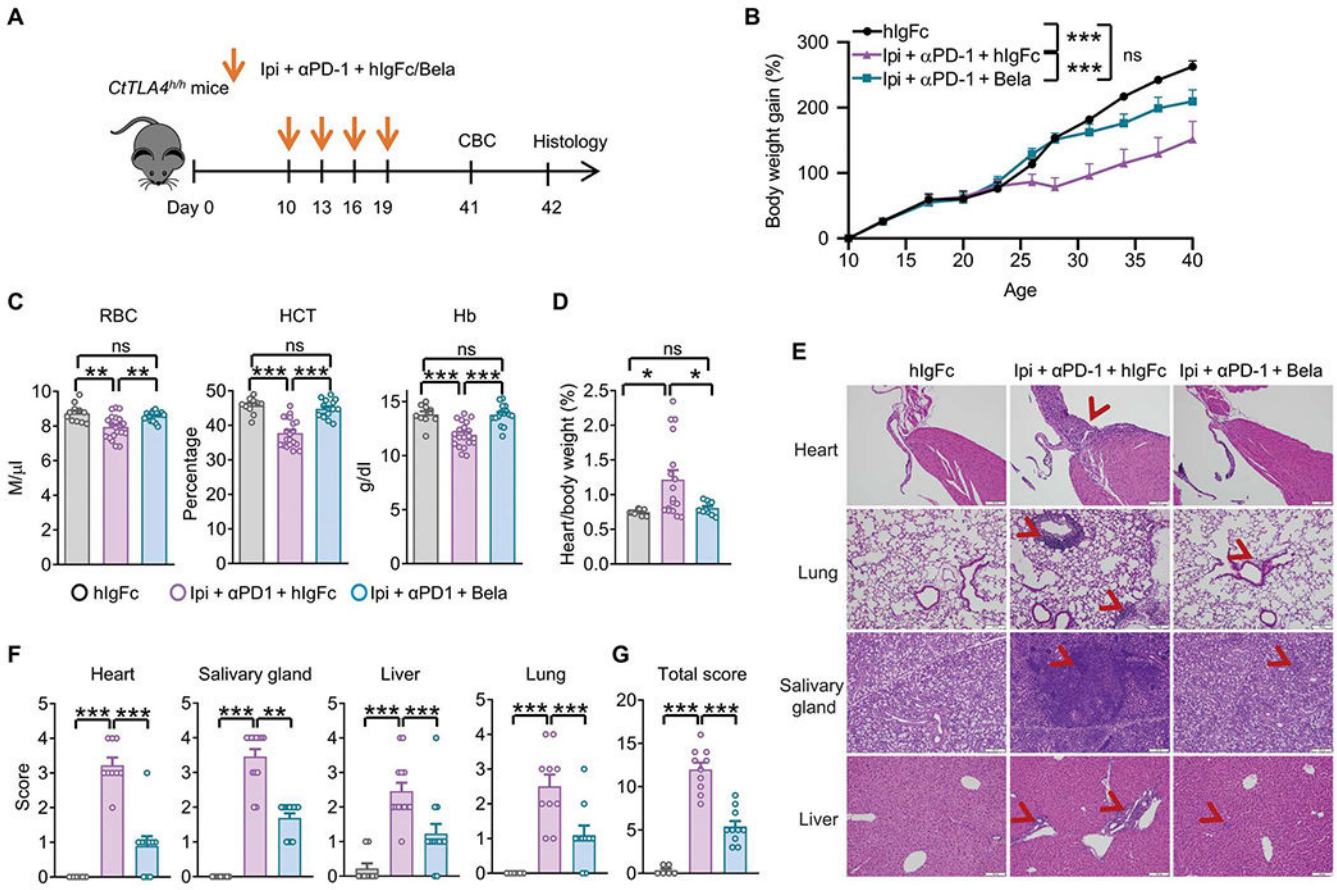

Fig. 4. Belatacept has a prophylactic effect on irAEs induced by ipilimumab and anti–PD-1 mAb treatment.

(**A**) Timeline of drug treatment and analysis. Ten-day-old *CTLA4*$^{h/h}$ mice were treated intraperitoneally with 100 μg of ipilimumab and 100 μg of anti–PD-1 mAb (RMP1-14) together with 100 μg of belatacept or hIgFc on days 10, 13, 16, and 19. The CBC analysis was performed on day 41, and necropsy was performed on day 42 after birth. (**B**) Body weight gain curves are shown for the indicated groups (n = 6 to 10 mice per group). One mouse from the ipilimumab and anti–PD-1 mAb-treated group was excluded from analysis because of death on day 28 with serious growth retardation. (**C**) Pure red cell aplasia was evaluated by RBC, HCT, and Hb analysis (n = 11 to 20 mice per group). (**D**) Heart weight (formalin-fixed) to body weight ratios of mice are shown (n = 10 to 17 mice per group). (**E**) Shown are representative images of H&E paraffin sections from the heart, lung, salivary gland, and liver. Representative inflammatory foci are marked with red arrowheads. Scale bars, 100 μm. (**F**) Toxicity scores of internal organs and glands based on inflammation are shown. (**G**) Composite scores of all organs and glands are shown. Data in (B) were analyzed by two-way repeated-measures ANOVA with Bonferroni's multiple comparison test. Data in (C), (D), (F), and (G) were analyzed by one-way ANOVA with Bonferroni's multiple comparisons test. Data are presented as means ± SEM. ns, $P \geq 0.05$; *$P < 0.05$; **$P < 0.01$; ***$P < 0.001$. Representative data of three independent experiments in (B) are shown. Data in (C) were combined from three experiments. Those in (D) to (G) were combined from two experiments.

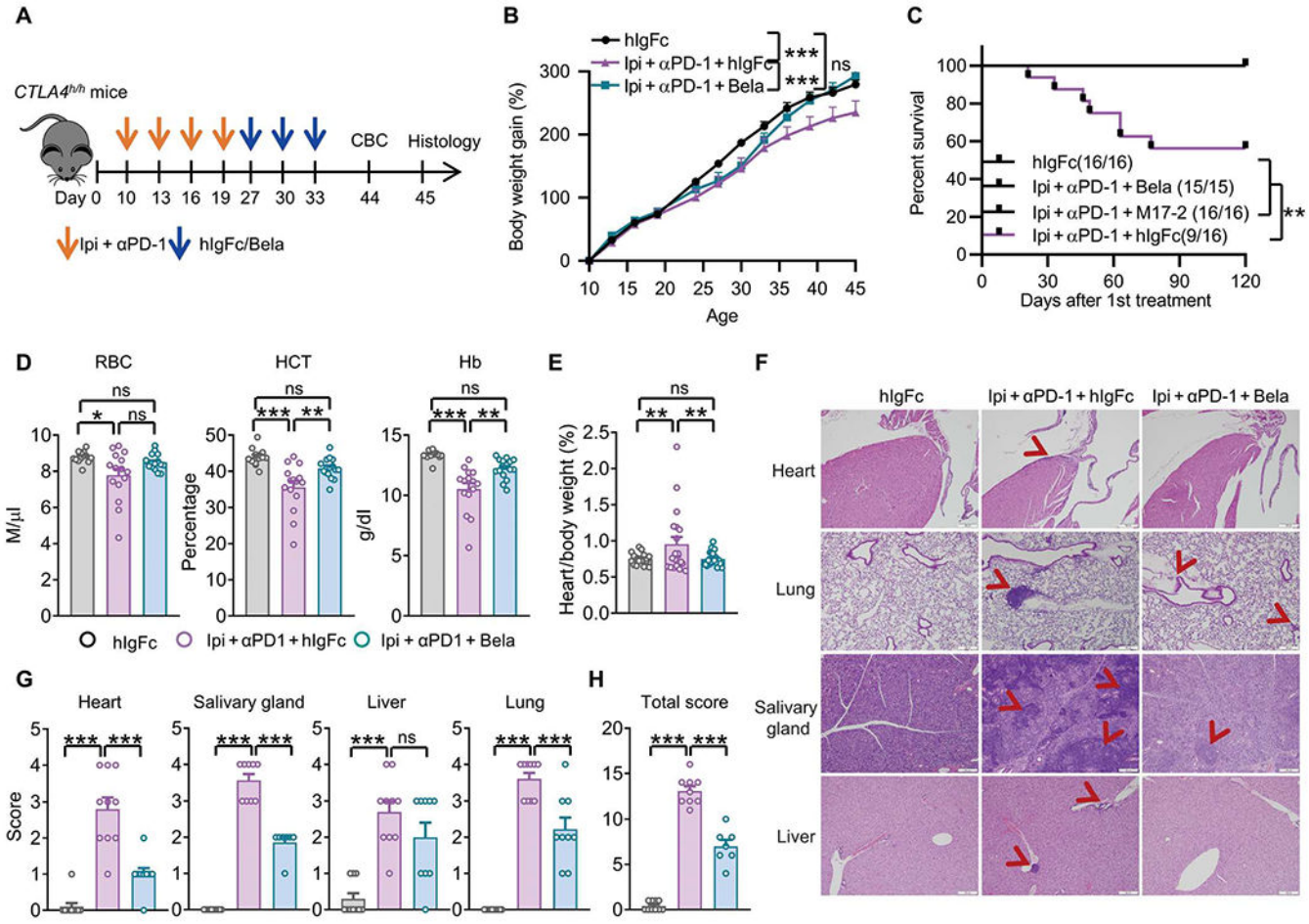

Fig. 5. Belatacept has a therapeutic effect on irAEs induced by ipilimumab and anti–PD-1 mAb treatment.

(**A**) Timeline of drug treatment and analysis. Ten-day-old *CTLA4*$^{h/h}$ mice were treated intraperitoneally with 100 μg of ipilimumab and 100 μg of anti–PD-1 mAb (RMP1-14) on days 10, 13, 16, and 19 and then treated with 100 μg of hIgFc or belatacept on days 27, 30, and 33. The CBC analysis was performed on day 44, and necropsy was performed on day 45. (**B**) Body weight gain ($n = 5$ mice per group) was monitored. (**C**) A survival curve is shown for the indicated groups. (**D**) Pure red cell aplasia was evaluated by RBC, HCT, and Hb analysis ($n = 13$ to 16 per group). (**E**) Heart weight (formalin-fixed) to body weight ratio of mice is shown ($n = 18$ to 20 per group). (**F**) Shown are representative images of H&E-stained paraffin sections from heart, salivary gland, liver, and lung. Representative inflammatory foci are marked with red arrowheads. Scale bars, 200 μm. (**G**) Shown are toxicity scores for internal organs and glands based on inflammation. (**H**) Composite scores are shown for all organs and glands. Data in (B) were analyzed by two-way repeated-measures ANOVA with Bonferroni's multiple comparison test. Data in (C) were evaluated with Kaplan-Meier survival analyses. Statistical significance of the *P* value was determined by log-rank test. (D), (E), (G), and (H) were analyzed by one-way ANOVA with Bonferroni's multiple comparisons test. Data are presented as means ± SEM. ns, $P \geq 0.05$; *$P < 0.05$; **$P < 0.01$; ***$P < 0.001$. Representative data of three independent

experiments in (B) are shown. Data in (C) to (E) were combined from three experiments. Those in (G) and (H) were combined from two experiments.

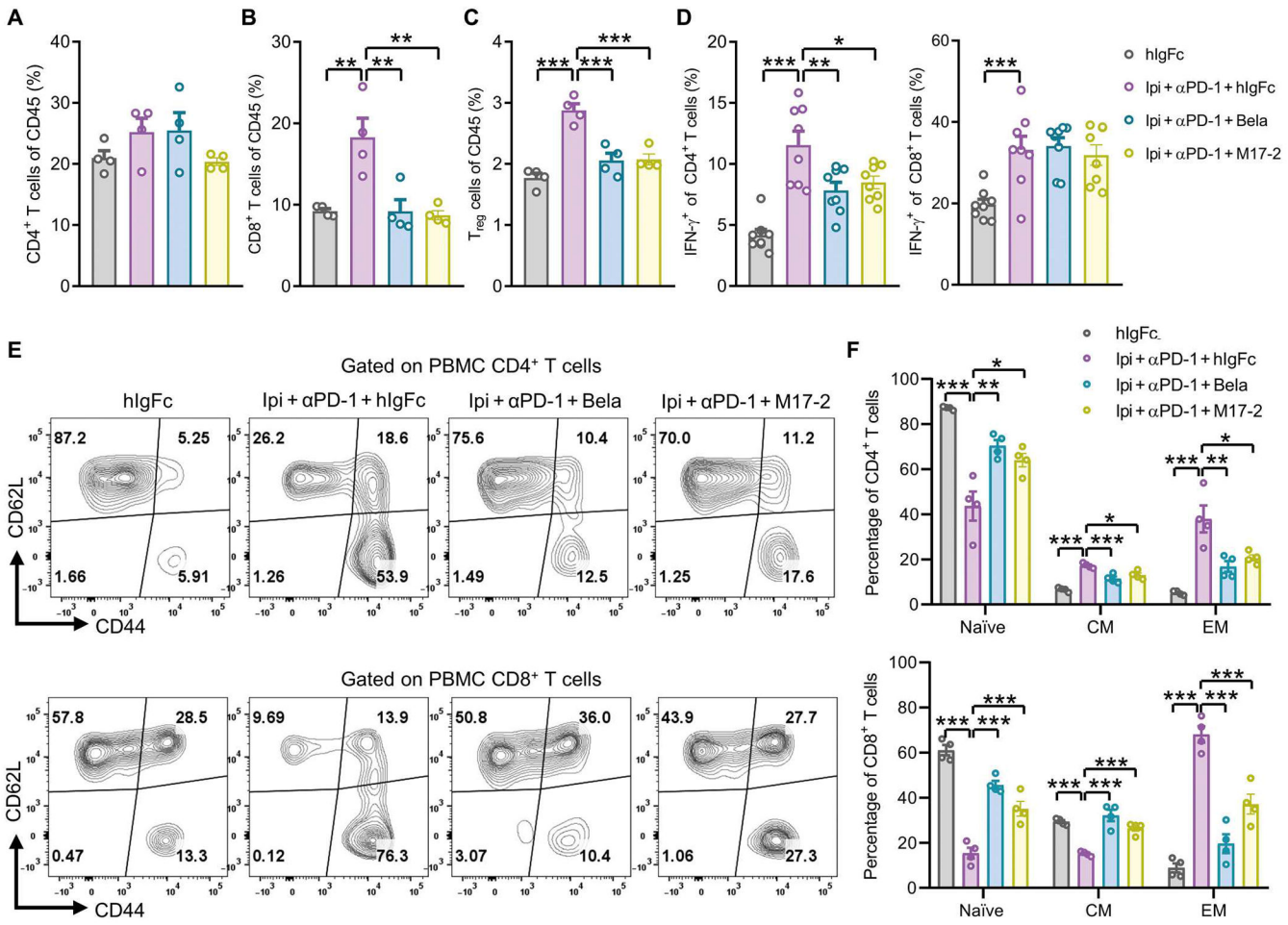

Fig. 6. CTLA-4 mutants reduce systemic T cell activation induced by ipilimumab and anti–PD-1 Ab treatment.

Ten-day-old *CTLA4*$^{h/h}$ mice were treated intraperitoneally with 100 μg of ipilimumab and 100 μg of anti–PD-1 mAb on days 10, 13, 16, and 19. Belatacept, M17-2, or hIgFc was administered on days 13, 16, 19, and 22. PBMCs were collected and evaluated by flow cytometry on day 31, and splenocytes were evaluated on day 45. (**A**) CD4$^+$ T cell, (**B**) CD8$^+$ T cell, and (**C**) T_{reg} frequencies of total CD45$^+$ cells are shown. (**D**) Intracellular staining of IFN-γ in CD4$^+$ and CD8$^+$ T cells after PMA and ionomycin stimulation is shown. The proportion of IFN-γ$^+$ cells within each population was quantified. (**E**) Representative flow cytometry plots depict naïve (CD44^{lo}CD62L^{hi}), central memory (CM;CD44^{hi}CD62L^{hi}), and effector memory (EM; CD44^{hi}CD62L^{lo}) CD4$^+$ (top) or CD8$^+$ (bottom) T cells. (**F**) Summary data are shown on the phenotypes of CD4$^+$ T cells (top) and CD8$^+$ T cells (bottom). Data were analyzed by one-way ANOVA with Bonferroni's correction for multiple comparisons. Data are presented as means ± SEM. *$P < 0.05$; **$P < 0.01$; ***$P < 0.001$. Representative data of at least two independent experiments are shown.

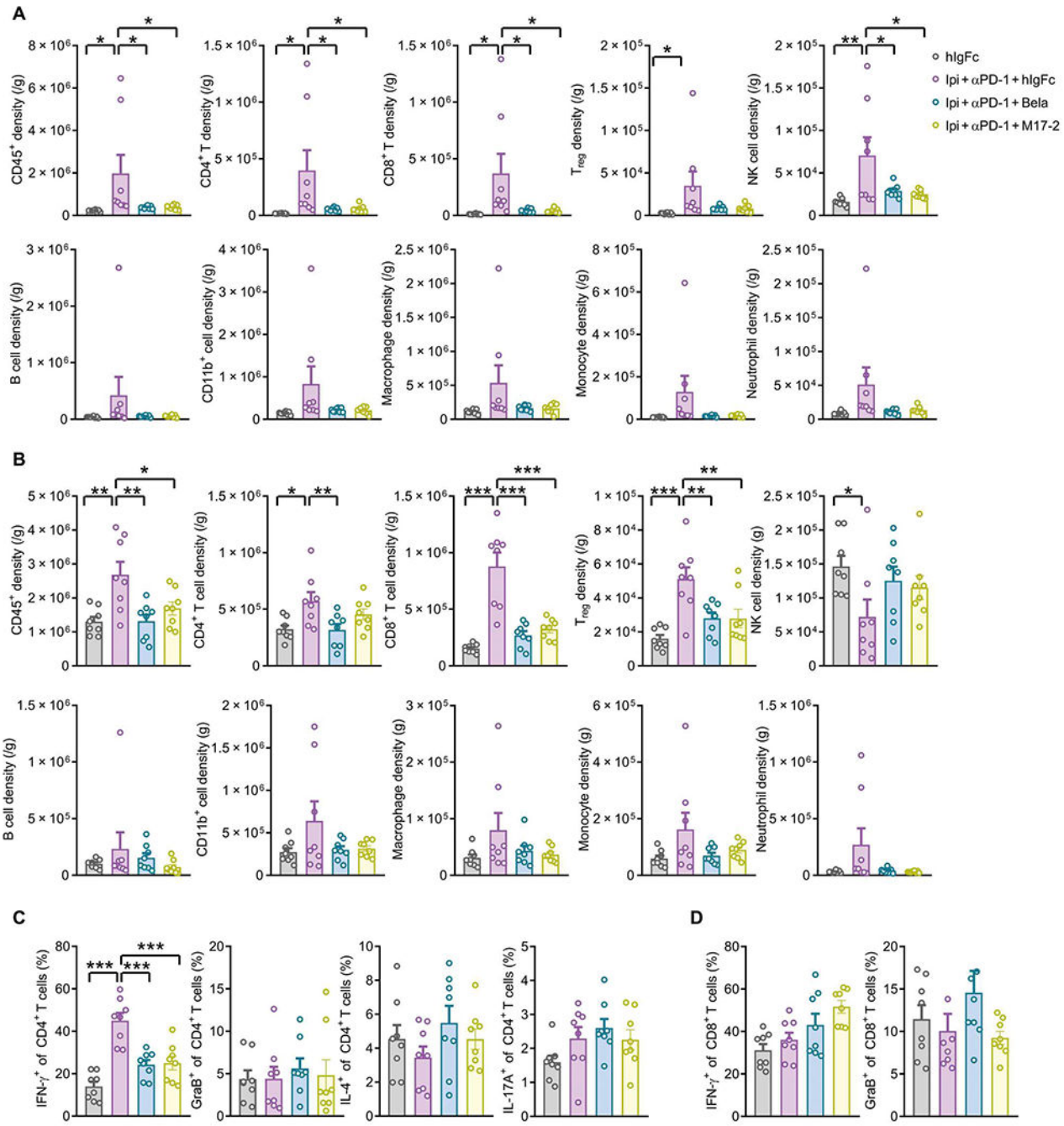

Fig. 7. CTLA-4 mutants reduce T cell infiltration and activation in irAE-targeted tissues.

Ten-day-old *CTLA4*$^{h/h}$ mice ($n = 8$) were treated intraperitoneally with 100 μg of ipilimumab and 100 μg of anti–PD-1 mAb on days 10, 13, 16, and 19. Belatacept, M17-2, or hIgFc was administered on days 13, 16, 19, and 22. Hearts and livers were collected for flow cytometry analysis on day 44 or 45. (**A**) Shown is the density of infiltrating immune cell populations in the heart. (**B**) Shown is the density of infiltrating immune cell populations in the liver. (**C** and **D**) Immune cells isolated from liver were stimulated with PMA and ionomycin together with brefeldin A blockade for 4 hours. Flow cytometry was used to

quantify intracellular cytokine and granzyme B abundance in $CD4^+$ T cells (C) and $CD8^+$ T cells (D). Data were analyzed by one-way ANOVA with Bonferroni's multiple comparisons test. Data are presented as means ± SEM. $*P < 0.05$; $**P < 0.01$; $***P < 0.001$. Data were combined from two independent experiments.